OsWOX13 functions as a heading signal transducer from integrator Ehd1 to florigen for the accurate regulation of rice heading date

Ming Yu[1], Minrui Chen[1,2], Xudong Zhu[1], Xinyue Zhang[1], Maohong Cai[1,2], Liang Zhou[1,2], Shirong Zhou[2], Chen Wang[2], Chao Li[2], Yimin Ling[1], Minxi Wu[1], Limin Zhang[1], Dekun Lei[1,2], Bingke Luo[1], Qiyu Yang[1], Wen Li[1,2], Xin Jin[1], Lizhuo Ma[1], Yulong Ren[1], Zhichao Zhao[1], Jie Wang[1], Cailin Lei[1], Zhijun Cheng[1], Qibing Lin[1], Xiuping Guo[1], Xin Wang[1], Shanshan Zhu[1,*], Jianmin Wan[1,2*]

[1] State Key Laboratory of Crop Gene Resources and Breeding, National Key Facility for Crop Gene Resources and Genetic Improvement, Institute of Crop Sciences, Chinese Academy of Agricultural Sciences, Beijing 100081, China

[2] State Key Laboratory for Crop Genetics & Germplasm Enhancement and Utilization, Nanjing Agricultural University, Zhongshan Biological Breeding Laboratory, Nanjing 210095, China

* Corresponding author, E-mail:

Jianmin Wan: wanjianmin@caas.cn, Shanshan Zhu: zhushanshan@caas.cn

The author responsible for distribution of materials integral to the findings presented in this article in accordance with the policy described in the Instructions for Authors (https://academic.oup.com/plcell/pages/General-Instructions) are Jianmin Wan (wanjianmin@caas.cn) and Shanshan Zhu (zhushanshan@caas.cn).

Short title：OsWOX13: Heading signal transducer in rice heading date regulation

Abstract

Appropriate heading date is an important safeguard for stabilizing rice yield and quality. Heading integrator Ehd1 and florigen Hd3a are crucial for rice heading. However, the mechanism by which Ehd1 transmits heading signals to Hd3a and the accurate regulation of *Hd3a* expression remains unclear. Here, we found that OsWOX13 functions as a signal transducer from Ehd1 to Hd3a for the accurate regulation of rice heading date. Ehd1 can directly bind to the *OsWOX13* promoter, OsWOX13 in turn binds to the *Hd3a* promoter to activate its expression. OsWOX13 interacts with Hd3a to inhibit OsWOX13-mediated activation of *Hd3a* expression, that precisely controls *Hd3a* levels. Meanwhile, late-heading phenotypes were observed in the *ehd1*, *Oswox13*, *Oswox13 ehd1*, *hd3a*, and *Oswox13 hd3a*, demonstrating that *Ehd1*, *OsWOX13*, and *Hd3a* coordinately regulate rice heading date. Furthermore, *OsWOX13* can be divided into two haplotypes, *Hap-T* and *Hap-C*. Ehd1 elevated *OsWOX13* expression in *Hap-T* compared with *Hap-C*. Longjing $31^{T\text{-}C}$ (carrying *Hap-C*) exhibited later heading dates than Longjing 31 (carrying *Hap-T*). Rice varieties carrying the *Hap-T* are predominantly cultivated in high-latitude regions. This study provides genetic resources and a theoretical foundation for improving the regional and climatic adaptability of rice.

Key words: rice, heading date, heading signal transducer, Ehd1, OsWOX13, Hd3a, haplotype

Introduction

Rice serves as a principal staple food crop, sustaining more than half of the global population (Zhang et al. 2025). Rice cultivation spans latitudes from 53°N to 40°S, with its regional adaptability primarily governed by heading date (Jung and Müller 2009). The heading date of elite cultivars must align with the local environmental conditions of a specific region, as both extremely early and delayed heading may lead to yield reduction (Huang et al. 2011; Huang et al. 2016). At present, global climate change is ongoing, and the heading date of rice is adjusted in a timely manner to accommodate the local climatic environment (Tao et al. 2013). To achieve this goal, research on the precision regulation of rice heading date is particularly necessary, and also serves as a pivotal underpinning for ensuring rice production adapts to climate change and achieves stable and increased yields.

In rice, the heading date is largely controlled by photoperiod sensitivity (Chen et al. 2018; Sun et al. 2023). The two primary photoperiodic pathways regulate heading date: the *GIGANTEA-Heading date 1-Heading date 3a/RICE FLOWERING LOCUS T 1* (*GI-Hd1-Hd3a/RFT1*) pathway and the *Early heading date 1* (*Ehd1*)-*Hd3a/RFT1* pathway, the latter of which is unique to rice (Cai et al. 2021). CONSTANS-like 4 (OsCOL4), OsCOL10, Days to heading on chromosome 8 (DTH8), Grains height date 7 (Ghd7), OsGhd7.1, and Hd16 repress heading through the inhibition of *Ehd1* expression (Xue et al. 2008; Lee et al. 2010; Wei et al. 2010; Hori et al. 2013; Gao et al. 2014; Tan et al. 2016), whereas Ehd2, Ehd4, Ehd5, OsMADS50, OsMADS51, and Hd17 facilitate heading date by enhancing *Ehd1* expression (Kim et al. 2007; Wu et al. 2008; Ryu et al. 2009; Matsubara et al. 2012; Gao et al. 2013; Zhang et al. 2023). The multiple upstream regulators of Ehd1 collect diverse heading signals, which are then converged at Ehd1 (Brambilla and Fornara 2013). Subsequently, Ehd1 integrates the heading signals and indirectly transmits them to the florigen genes *Hd3a/RFT1* that are crucial for the heading date in rice (Komiya et al. 2008; Tsuji et al. 2010). However, it remains unclear through which specific protein Ehd1 transmits the heading signal to florigen genes and how it precisely controls the expression of these genes.

Heading date is a typical quantitative trait controlled by multiple genes in rice. To date, haplotypes of several heading date-regulating genes have been identified, including *DTH8*, *Ghd7*, *Hd1*, *DTH7*, *PhyB*, and *OsCOL4*. In a panel of 148 rice accessions, *DTH8*, *Ghd7*, *Hd1*, *DTH7*, *PhyB*, and *OsCOL4* harbored 25, 47, 41, 59, 30, and 19 single nucleotide polymorphisms (SNPs), respectively (Cui et al. 2020). Most of these SNPs led to amino acid (aa) substitutions, and the majority of functionally significant mutations were located in the first exon. Three, two, one, and five SNPs causing premature stop codons were detected in *DTH8*, *DTH7*, *Ghd7*, and *Hd1*, respectively. In addition, 3, 4, 2, 6, 3, and 1 insertion-deletion (InDel) loci were identified in these six genes in the same order. Subsequent haplotype analysis revealed 18, 41, 41, 42, 28, and 22 distinct haplotypes for *DTH8*, *Ghd7*, *Hd1*, *DTH7*, *PhyB*, and *OsCOL4*, respectively. The genetic diversity of these genes has been of great significance for the expansion of rice cultivation into high-latitude regions (Zheng et al. 2016). Nevertheless, breeding rice varieties with broad regional adaptability still requires the identification and application of more haplotypes of heading date-associated genes, as well as in-depth dissection of their molecular regulatory mechanisms.

WUSCHEL-Related Homeobox (*WOX*) genes are plant-specific, and their encoded WOX proteins constitute a large family (Van et al. 2009). The most prominent structural feature of WOX transcription factors is the homeodomain, a highly conserved region that forms the DNA-binding domain (Muhammad et al. 2022). It consists of three α-helices, in which the second and third helices form a helix-turn-helix motif responsible for recognizing and binding specific DNA sequences within the promoter regions of target genes (Lian et al. 2014). The conservation of the homeodomain across different plant species underscores its central role in the functional execution of WOX proteins (Han et al. 2021). As a molecular anchoring site, it enables WOX transcription factors to interact with DNA and initiate transcriptional regulation. The homeodomain of the WOX protein family contains 65 amino acid residues, while some atypical WOX homeodomains bear additional residues (Mukherjee et al. 2009). This family is classified into three clades: the modern, intermediate, and ancient branches and is widely involved in the regulation of various aspects of plant growth and development (Van et al. 2009). In *Arabidopsis thaliana*, the *atwox13* mutant exhibits early flowering compared to the wild type, whereas the *atwox14* mutant displays delayed flowering relative to the wild type (Deveaux et al. 2008). *OsWOX5* and *OsWOX10* exert opposing roles in the regulation of lateral root primordium development in rice (Kawai et al. 2022). Overexpression of *OsWOX5* promotes an increase in lateral root diameter, whereas mutation in *OsWOX10* leads to a reduction in lateral root diameter. OsWOX11 enhances the transcription of *lateral organ boundaries domain 16* (*LBD16*) by binding to its promoter and interacting with JMJ706 (Geng et al. 2024). Conversely, the interaction between OsWOX11 and LBD16 inhibits the OsWOX11-JMJ706 interaction, thereby reducing *LBD16* transcription. This regulatory mechanism controls crown root development. OsWOX13 can promote rice heading, but its molecular and genetic regulatory mechanisms remain unclear (Minh-Thu et al. 2018; Kim 2024). Meanwhile, *OsWOX13* is the only gene belonging to the ancient clade of the rice *WOX* family, which is the most conserved clade with generally few haplotypes (Deveaux et al. 2008). Therefore, exploring the molecular and genetic mechanisms by which *OsWOX13* and its haplotypes regulate rice heading date is of great significance for the precise regulation of rice heading date.

In this study, chromatin immunoprecipitation sequencing (ChIP-Seq) analysis, along with both in vitro and in vivo binding assays, demonstrated that Ehd1 can bind to the promoter of *OsWOX13* and thereby activate its expression. We also found that OsWOX13 promotes the

expression of *Hd3a* by directly binding to its promoter. OsWOX13 can physically interact with Hd3a, and the interaction reduces OsWOX13-mediated activation of *Hd3a* expression. Late-heading phenotypes were observed in *ehd1*, *Oswox13*, *Oswox13 ehd1*, *hd3a* and *Oswox13 hd3a* mutants, suggesting that *Ehd1*, *OsWOX13* and *Hd3a* co-regulate rice heading date. Additionally, Ehd1 elevated the expression of *OsWOX13* in *Hap-T* relative to *Hap-C*, alongside downstream *Hd3a*, thereby modulating rice heading date. Rice harboring the *Hap-T* was selected during domestication and cultivated in high-latitude regions. Our study demonstrated that *OsWOX13* responds to Ehd1, transmits the heading signal to Hd3a, and precisely regulate its expression levels. Additionally, our study investigated the molecular mechanisms by which different *OsWOX13* haplotypes influence rice cultivation regions, thereby providing a theoretical basis and genetic resources for improving the regional adaptability of rice varieties.

Results

Ehd1 directly regulates the expression of *OsWOX13*

To identify genes directly regulated by Ehd1, the Ehd1-FLAG overexpression lines *(Ehd1-OE*) and *ehd1* mutants were first obtained. The expression of *Ehd1* and its protein levels in *Ehd1-OE* were significantly higher than those in Nipponbare (NIP) (Supplementary Fig. S1, A and B). Furthermore, the *Ehd1-OE* exhibited early heading phenotype, whereas the *ehd1* mutants showed delayed heading relative to NIP under natural long-day (NLD) and natural short-day (NSD) conditions (Supplementary Fig. S2, A to E). Meanwhile, compared with NIP, the *Ehd1-OE* exhibited increased grain number per panicle and number of secondary branches per panicle, as well as decreased plant height, panicle length, grain length and grain width (Supplementary Table S1). In contrast, the *ehd1* mutants showed reduced plant height, grain number per panicle, fruit set rate per panicle, number of secondary branches per panicle, panicle length, 1000-grain weight and grain width. Furthermore, ChIP-Seq analysis was performed using *Ehd1-OE-1* (Supplementary Table S2 to S4). To validate the reliability of ChIP-Seq, we screened enriched DNA fragments located in gene promoter regions and randomly selected five regions with high enrichment scores for experimental verification. ChIP-qPCR assays were performed using the *Ehd1-OE-1* and *ProEhd1:Ehd1-GFP ehd1-2* lines to re-examine five gene promoters that were potentially bound by Ehd1 in the ChIP-Seq data (Supplementary Fig. S3). In the *Ehd1-OE-1* and *ProEhd1:Ehd1-GFP ehd1-2* lines, the significant enrichment of these five gene promoters by

Ehd1 confirmed the accuracy of the ChIP-Seq results (Supplementary Fig. S4, A and B). To determine whether the five genes are involved in the regulation of heading date in rice, mutants of these five genes were constructed via CRISPR-Cas9 (Supplementary Fig. S4C). Unfortunately, there are no obvious heading data and other agronomic traits differences between NIP and these mutants under NLD and NSD conditions (Supplementary Fig. S4, D and E; Table S1). We performed a phylogenetic analysis (Supplementary Fig. S5), which revealed that four of the proteins (LOC_Os02g46860, LOC_Os06g08350, LOC_Os03g61200, and LOC_Os12g01410) belong to multi-member families in rice that share identical conserved functional domains, and LOC_Os01g13090 is part of a tandem duplication. Thus, the single mutants of these five genes exert no obvious effects on the growth and development of rice.

To further identify genes directly regulated by Ehd1 in the heading date pathway, we further analyzed the ChIP-Seq data and found a significant enrichment peak of Ehd1 at the *P2* region of the *OsWOX13* promoter (contained a 105 bp upstream sequence of the ATG start codon, including 72 bp downstream fragment) (Fig. 1A; Supplementary Fig. S6). The *WOX* gene family is unique to plants and is involved in regulating various growth and developmental processes in rice (Han et al. 2021). In rice, *OsWOX13* is the only gene in the ancient clade of the *WOX* gene family and may possess more conserved functions (Deveaux et al. 2008). Meanwhile, *OsWOX13* has been reported to regulate rice heading date, but its molecular and genetic mechanisms remain unclear (Minh-Thu et al. 2018). To further dissect the mechanism by which *OsWOX13* regulates rice heading date, the binding of Ehd1 to the *OsWOX13* promoter was further verified. Furthermore, ChIP-qPCR assays showed that Ehd1 significantly enriched the *OsWOX13-P2* region in both the *ProEhd1:Ehd1-GFP ehd1-2* and *Ehd1-OE-1* lines (Fig. 1B; Supplementary Fig. S7). To further define the binding specificity of Ehd1 on a genome-wide scale, we performed genome-wide motif enrichment analysis using all ChIP-Seq peaks and identified the top 10 de novo homer motifs as well as the top 10 known motifs, thereby providing a detailed view of the conserved DNA motifs recognized by Ehd1 at the genomic level (Supplementary Fig. S8). In addition, we performed separate motif analysis specifically on the Ehd1-binding peaks within the *OsWOX13* promoter region (Fig. 1C). However, the precise position of the Ehd1-binding motif was not identified. To identify the *Ehd1*-binding site in the *OsWOX13* promoter, *OsWOX13-P2* was equally divided into four fragments with a 9 bp overlap between adjacent ones, which were designated as *OsWOX13-P2-1*, *OsWOX13-P2-2*, *OsWOX13-P2-3*,

and *OsWOX13-P2-4*, respectively (Fig. 1A). Electrophoretic mobility shift assay (EMSA) showed GST-Ehd1 only exhibited a clear binding band with the labeled probe (*OsWOX13-P2-2*), which progressively weakened with the addition of competitive probes (Supplementary Fig. S9, A to D). In contrast, GST failed to bind to *OsWOX13-P2-2*. Subsequently, *OsWOX13-P2-2* was equally divided into three fragments: *OsWOX13-P2-2-1*, *OsWOX13-P2-2-2* and *OsWOX13-P2-2-3*, with a 10 bp overlap between adjacent fragments (Fig. 1A). But, GST-Ehd1 failed to bind to any of the three labeled probes (Supplementary Fig. S9, E to G). This suggests that Ehd1 might require extended DNA sequences for effective binding. To further confirm that Ehd1 bind to the *OsWOX13-P2-2* region, we designed two mutation probes (mut probe-T/-G) of *OsWOX13-P2-2* targeting the overlapping regions of *OsWOX13-P2-2-1* and *OsWOX13-P2-2-2*, or *OsWOX13-P2-2-2* and *OsWOX13-P2-2-3* (Fig. 1A). The binding intensities of GST-Ehd1 to mut probe-T and mut probe-G were diminished compared to those observed with labeled probe *OsWOX13-P2-2* (Fig. 1D). Furthermore, a dual-luciferase reporter (LUC) assay was performed, and demonstrated that Ehd1 significantly enhanced the transcriptional activity of the *OsWOX13-P1* (contained a 2000 bp upstream sequence of the ATG start codon, including 72 bp downstream fragment identified) and its sub-fragment *OsWOX13-P2* (Fig. 1E; Supplementary Fig. S10). Meanwhile, The LUC assay showed that Ehd1 significantly enhanced the transcriptional activity of *OsWOX13-P2-2*. Consistently, the transcriptional activation activity exhibited a declining trend in *OsWOX13-P2-2-Mut-G* and *OsWOX13-P2-2-Mut-T*. Thus, all these data suggest that Ehd1 directly binds to the *OsWOX13* promoter both in vivo and in vitro.

To characterize the expression patterns of *Ehd1* and *OsWOX13*, we analyzed their transcript levels in various tissues. Both genes were expressed in leaves, stems, spikes, leaf sheaths and roots (Supplementary Fig. S11, A and B). In situ hybridization assays were performed in rice stems at 40-, 45-, and 50- days growth stages. Signals of *Ehd1* and *OsWOX13* in stem tissues at the same stages were stained purple by NBT (Supplementary Fig. S11C). Furthermore, in situ hybridization assays were performed on leaf tissues from NIP at the 25-, 30- and 35-day growth stages (Supplementary Fig. S11D). The hybridization signals of *OsWOX13* were first stained red with Fast Red, followed by subsequent staining of *Ehd1* signals with NBT to yield purple color on the identical leaves. No specific staining signal was observed in the control stems and leaves. In leaves of NIP, *OsWOX13* exhibited a rhythmic expression pattern within 48-hour period (Fig. 1, F and G). Under NLD and CSD conditions, the expression levels of *OsWOX13* gene began to

increase before dawn, reached its peak within four hours after dawn, and then started to decline (Fig. 1, F and G). The rhythmic expression pattern of *OsWOX13* was similar to that of *Ehd1* (Itoh et al. 2010). Meanwhile, the protein levels of OsWOX13 was expressed throughout the day (Supplementary Fig. S12). Furthermore, *OsWOX13* expression was higher in *Ehd1-OE* than in NIP, whereas its expression was lower in *ehd1* mutants compared with NIP under NLD and CSD conditions (Fig. 1, F and G). Collectively, these results demonstrated that *Ehd1* and *OsWOX13* exhibited spatiotemporally coincident expression in leaves and stems and a similar rhythmic expression pattern, and that Ehd1 could activate the expression of *OsWOX13*.

OsWOX13 and _Ehd1_ coordinately regulate heading date

To elucidate the function of *OsWOX13*, we generated two CRISPR/Cas9 targets for *OsWOX13* and generated three distinct mutants (Fig. 2A). Additionally, we constructed four independent *OsWOX13* overexpression lines (*OsWOX13-OE*) (Supplementary Fig. S13, A and B). Compared with NIP, *OsWOX13-OE-1*, *-2*, *-3* and *-4* exhibited earlier heading date under both NLD and NSD conditions (Fig. 2, B to E). In contrast, the heading date of *Oswox13-1*, *-2* and *-3* mutants was delayed by approximately 3 days under NLD conditions and by approximately 8 days under NSD conditions. The findings indicated that *OsWOX13* facilitated rice heading.

Meanwhile, the *OsWOX13* was also found to regulate several agronomic traits. The *OsWOX13-OE* exhibited greater 1000-grain weight but had less plant height, fewer grain number per panicle, number of secondary branches per panicle, panicle length and grain width compared with NIP (Supplementary Table S1). Relative to the NIP, the *Oswox13* exhibited enhanced tiller number, while displaying significant reductions in plant height, grain number per panicle, fruit set rate per panicle, secondary branch number per panicle, panicle length, 1000-grain weight and grain width.

To elucidate the genetic relationship between *OsWOX13* and *Ehd1*, the *Oswox13 ehd1* double mutant was generated (*Oswox13-2 ehd1-1* and *Oswox13-3 ehd1-2*). Under NLD and NSD conditions, all *ehd1-1*, *Oswox13-2*, *Oswox13-2 ehd1-1* and *Oswox13-3 ehd1-2* showed late heading date, compared with NIP. (Fig. 2, F to H). These results indicated that *OsWOX13* and *Ehd1* coordinately regulated rice heading date. Meanwhile, plant height, fruit set rate/panicle, 1000-grain weight, and grain width were further reduced in *Oswox13 ehd1* (Supplementary Table S1). The tiller number, which was decreased in the *ehd1*, was restored in the *Oswox13 ehd1*,

similar to the *Oswox13*. The grain number per panicle and secondary branch number in the *Oswox13 ehd1* were similar to those in *Oswox13* or *ehd1*, and the panicle length in the *Oswox13 ehd1* recovered to the level of NIP. These results suggest that *OsWOX13* and *Ehd1* share a certain genetic relationship in the regulation of other agronomic traits.

OsWOX13 interacts with the promoter of *Hd3a*

To identify downstream genes regulated by OsWOX13, a nuclear-localized transcription factor (Supplementary Fig. S14), within the heading date regulatory network, we conducted transcriptome sequencing on NIP, *OsWOX13-OE-1* and *Oswox13-2*. KEGG enrichment analysis on NIP, *Oswox13-2* and *OsWOX13-OE-1* showed five genes involved in the heading date pathway were differentially expressed (Supplementary Fig. S15A). Among the differentially expressed genes, the expression patterns of *PHYA-like* and *OsELF3.2* did not align with the observed heading-date phenotypes in *OsWOX13* transgenic plants (Xu et al. 2023) (Supplementary Fig. S15B). In contrast, *Hd3a* expression was consistently upregulated in the *OsWOX13-OE* line and downregulated in the *Oswox13* mutant, showing the most pronounced change (Supplementary Fig. S15C). Furthermore, promoter analysis revealed that *Hd3a* is the only gene among them that contains the reported OsWOX13-binding motif (CAATCAAT) in its promoter region (Minh-Thu et al. 2018) (Fig. 3A). This combination of expression correlation and the presence of a specific *cis*-element led us to select *Hd3a* for further functional validation. The full-length 2500 bp promoter of the *Hd3a* gene was designated as *Hd3a-P1*, while the 100 bp region and the 30 bp region containing the CAATCAAT motif were named *Hd3a-P2* and *Hd3a-P3*, respectively (Fig. 3A). The LUC assay showed that the transcriptional activity of *Hd3a-P1* and *Hd3a-P2* was significantly higher with OsWOX13-FLAG as the effector than with the FLAG-only control (Fig. 3, B and C). ChIP-qPCR analysis was performed using *ProOsWOX13: OsWOX13-FLAG Oswox13-2* and *OsWOX13-OE-1* lines (Supplementary Fig. S16), showed that the DNA region of *Hd3a-P2* was significantly enriched by OsWOX13, in comparison with the control group (Fig. 3D; Supplementary Fig. S17). Furthermore, EMSA assays showed His-OsWOX13 specifically bound to the biotin-labeled probe, forming a distinct band (Fig. 3E). In contrast, the His protein showed no binding. The binding band weakened progressively with the addition of a competitor, and no binding was detected with the mutant probe. These results illustrated that OsWOX13 directly bound to the *Hd3a* promoter.

The regulatory pattern of OsWOX13 on *Hd3a* expression

Hd3a was expressed in leaf, stem, spike, leaf sheath and root (Supplementary Fig. S18A). Moreover, we performed in situ hybridization assays using leaf tissues isolated from NIP at the 25-, 30- and 35-day growth stages (Supplementary Fig. S18B). For dual signal detection on the same leaf sections, *OsWOX13* signals were first stained red with Fast Red, and *Hd3a* signals were then labeled purple by NBT staining. *OsWOX13* and *Hd3a* exhibited overlapping in situ hybridization signals in leaf tissues. In contrast, no specific hybridization signals were observed in the leaves of control. Furthermore, the expression patterns of the *Hd3a* gene over a 48-hour period under NLD and CSD conditions were examined in leaves of NIP, *OsWOX13-OE* and *Oswox13*. The *Hd3a* expression was elevated in *OsWOX13-OE* compared to NIP during the period from dawn to dusk, while it was reduced in *Oswox13* compared to NIP. In other time periods, the expression levels of *Hd3a* remained consistently low across NIP, *OsWOX13-OE*, and *Oswox13* (Fig. 3, F and G). Meanwhile, the expression levels of *Ehd1* showed no significant difference between NIP, *OsWOX13-OE* and the *Oswox13* (Supplementary Fig. S19). Subsequently, compared with NIP, the expression level of *hd3a* was decreased in the *Oswox13*, while the expression level was further reduced in the *Oswox13 ehd1*, which was consistent with that in the *ehd1* (Supplementary Fig. S20, A and B). Ehd1 was transiently overexpressed in protoplasts of *Oswox13* and NIP. Compared with *Oswox13* protoplasts, the expression level of *Hd3a* was increased in *Ehd1* overexpressed *Oswox13* protoplasts, and a further increase was observed in *Ehd1* overexpressed NIP protoplasts (Supplementary Fig. S20C). Taken together, these findings confirmed that *Hd3a* and *OsWOX13* displayed spatiotemporally overlapping expression patterns with consistent rhythmicity (Itoh et al. 2010). Moreover, OsWOX13, as one of the intermediate factors in the Ehd1-mediated regulation of *Hd3a* expression, can activate *Hd3a* expression, possibly independently of *Ehd1*.

Hd3a interacted with OsWOX13 to repress its own expression activation

Hd3a, as a florigen protein in rice, plays a crucial role in determining the heading date (Komiya et al. 2008; Tsuji et al. 2010). How *Hd3a* expression is precisely regulated is a crucial issue, which determines the optimal time for rice heading. Here, we found that Hd3a physically interacted with OsWOX13 (Fig. 4, A to C). Through the bimolecular fluorescence complementation experiment, we observed a distinct fluorescent signal in the nuclei of *Nicotiana*

benthamiana leaves transiently co-infiltrated with the OsWOX13-nYFP and Hd3a-cYFP constructs, whereas no fluorescent signal was detected in the two control groups (Fig. 4A). Further, the pull-down assay demonstrated that His-OsWOX13 specifically bound to GST-Hd3a, not GST alone (Fig. 4B). In the co-immunoprecipitation (Co-IP) experiment, OsWOX13-FLAG selectively bound to Hd3a-GFP (Fig. 4C). These results illustrated that Hd3a and OsWOX13 interacted both in vivo and in vitro, and the interaction occurred in the nucleus.

To explore the interaction region between OsWOX13 and Hd3a, OsWOX13 was truncated into three fragments according to its domain structure (Supplementary Fig. S21A). Hd3a interacted with OsWOX13$^{1\text{-}90\ \text{amino acid (aa)}}$ and OsWOX13$^{151\text{-}268\ \text{aa}}$ (Supplementary Fig. S21, B and C), but not with OsWOX13$^{91\text{-}150\ \text{aa}}$ (Supplementary Fig. S21, C and D). Furthermore, OsWOX13, OsWOX13$^{1\text{-}90\ \text{aa}}$ and OsWOX13$^{151\text{-}268\ \text{aa}}$ were found to exhibit transcriptional activation activity in yeast (Supplementary Fig. S21D). Subsequently, a LUC assay was performed. For the transient expression assays conducted in *hd3a-1* protoplasts, *Pro35S:Gal4BD*, *Pro35S:OsWOX13-Gal4BD*, *Pro35S: OsWOX13$^{1\text{-}90\ aa}$-Gal4BD*, *Pro35S:OsWOX13$^{91\text{-}150\ aa}$-Gal4BD*, *Pro35S:OsWOX13$^{151\text{-}268\ aa}$-Gal4BD*, *Pro35S:GFP*, and *Pro35S:Hd3a-GFP* were used as effectors, while the *Pro35S:*REN-*UAS*-LUC construct served as the reporter (Supplementary Fig. S21E). The LUC assay results showed that OsWOX13, OsWOX13$^{1\text{-}90\ \text{aa}}$ and OsWOX13$^{151\text{-}268\ \text{aa}}$ were confirmed to possess transcriptional activation activity in vivo, while OsWOX13$^{91\text{-}150\ \text{aa}}$ showed no such activity (Supplementary Fig. S21F). In addition, Hd3a was able to repress the transcriptional activation capacity of OsWOX13, OsWOX13$^{1\text{-}90\ \text{aa}}$ and OsWOX13$^{151\text{-}268\ \text{aa}}$.

To explore the effect of Hd3a-OsWOX13 on the interaction between OsWOX13 and *Hd3a* promoter, a LUC assay was performed. For the transient expression assays conducted in *hd3a-1* protoplasts, *Pro35S:FLAG*, *Pro35S:OsWOX13-FLAG*, *Pro35S:GFP*, and *Pro35S:Hd3a-GFP* were used as effectors, while the *Pro35S:*REN-*Hd3a-P1*-LUC construct served as the reporter (Fig. 4D). It was observed that *Pro35S:Hd3a-GFP* significantly inhibited the activity of OsWOX13 in activating *Hd3a-P1* (Fig. 4E). However, this inhibition did not completely abolish the activation capacity of *Pro35S:OsWOX13-FLAG* on *Hd3a-P1*. Furthermore, protoplasts of NIP and the *hd3a* mutant were isolated and transiently transformed with *ProOsWOX13:OsWOX13-FLAG*, followed by ChIP-qPCR assays (Fig. 4F). The results showed that OsWOX13 was significantly enriched at the *Hd3a-P2* region, and the enrichment rate was

higher in the *hd3a-1* than in NIP. Concurrently, EMSA experiments demonstrated that Hd3a could not bind the *Hd3a-P3* labeled probe. However, it weakened the binding of OsWOX13 to the *Hd3a-P3* labeled probe (Fig. 4G). Meanwhile, NIP protoplasts were co-transformed with either OsWOX13-FLAG+GFP (control group) or OsWOX13-FLAG+Hd3a-GFP (experimental group) (Fig. 4H). *OsWOX13* expression levels were comparable between the two groups, whereas endogenous *Hd3a* transcription was significantly repressed in the experimental group. Meanwhile, the circadian rhythm of *Hd3a* expression was examined in NIP and the *hd3a-1*. The results showed that the oscillation amplitude of *Hd3a* was much lower in the *hd3a*-1 than in NIP (Fig. 4I). Taken together, *OsWOX13*-mediated transcriptional activation of *Hd3a* was attenuated via interaction between OsWOX13 and Hd3a, which precisely modulated *Hd3a* expression.

Convergent regulation of rice heading date by *OsWOX13* and *Hd3a*

To elucidate the genetic relationship between *Hd3a* and *OsWOX13* in regulating rice heading date, the *hd3a* mutant from a previous study (Zhu et al. 2017), as well as the newly generated *Oswox13-2 hd3a-1* and *Oswox13-2 hd3a-2* double mutants, were used in this research (Fig. 5A). Under long-day conditions, the heading date phenotypes of the *Oswox13-2* single mutant, *Oswox13-2 hd3a-1*, and *Oswox13-2 hd3a-2* double mutants were consistent with those of the *hd3a-1* single mutant, all exhibiting significantly delayed heading compared to the NIP (Fig. 5, B and C). Under short-day conditions, the *hd3a-1* single mutant exhibited a later heading date than the *Oswox13-2* single mutant, but its heading date was consistent with those of the *Oswox13-2 hd3a-1* and *Oswox13-2 hd3a-2* double mutants (Fig. 5D). Furthermore, we overexpressed *OsWOX13* in the *hd3a-1*, generating lines *OsWOX13-OE*-3 *hd3a-1* and *OsWOX13-OE-4 hd3a-1* (Supplementary Fig. S22). Overexpression of *OsWOX13* in the *hd3a-1* mutant did not significantly rescue the late-heading phenotype (Fig. 5, E to G). These results indicated that *OsWOX13* and *Hd3a* coordinately regulated heading date in rice, with *Hd3a* being the downstream gene of *OsWOX13* in this regulation.

Meanwhile, the *Oswox13* and *hd3a* exhibited decreased plant height, while the *Oswox13 hd3a* showed partial recovery in plant height. Moreover, plant height in *OsWOX13-OE hd3a* was further reduced compared with the *hd3a* mutant. Tillering number in the *Oswox13 hd3a* and *OsWOX13-OE hd3a* lines was significantly higher than that in the *hd3a*. In contrast, grain number per panicle, number of secondary branches per panicle, panicle length, and 1000-grain

weight were significantly lower than those in *hd3a*. Fruit set rate per panicle in the *Oswox13 hd3a* was further reduced relative to *Oswox13*, and that in *OsWOX13-OE hd3a* was lower than in *hd3a*. Grain length and width in the *Oswox13 hd3a* were slightly decreased compared with the *hd3a* (Supplementary Table S1). These results suggest that *OsWOX13* and *Hd3a* share a certain genetic relationship in the regulation of other agronomic traits.

Natural variation in *OsWOX13* promoted heading date in rice and its geographic distribution

To investigate the impact of natural variation in *OsWOX13* on heading date in germplasm resources, we analyzed its allelic variation using the rice functional genomics and breeding database version 2.0 (Wang et al. 2018). We found that variations in *OsWOX13* were primarily located in the untranslated region (UTR) and the first intron regions, with only a single base mutation from G to A in the second exon (Supplementary Table S5). However, this mutation did not result in an amino acid change, suggesting that OsWOX13 is a highly conserved transcription factor. Interestingly, we identified a single nucleotide polymorphism (SNP) within the *P2-2* region of the *OsWOX13* promoter, which is the binding site for Ehd1 (Supplementary Table S5). *OsWOX13-P2-2* spans the region from 12 to 63 bp upstream of the *OsWOX13* ATG start codon, and this SNP is situated at the 54th base within this region. Based on this SNP, the *OsWOX13* gene was categorized into two homozygous haplotypes and one heterozygous genotype: *Hap-C* (homozygous for cytosine (C) at Chr1:34863184), *Hap-T* (homozygous for thymine (T) at the identical genomic position), and *Hap-Y* (heterozygous T/C at the same site). The total number of varieties was 2792. The frequencies of the *Hap-T* and *Hap-C* were 33.7% and 64.4%, respectively, whereas *Hap-Y*, corresponding to the heterozygous genotype, exhibited a frequency of 1.9% (Fig. 6A). The average heading date of *Hap-C* rice was 95.974 days, significantly later than that of *Hap-T* rice (Fig. 6A). To further clarify the effect of this SNP within the *P2-2* region of the *OsWOX13* promoter on heading date, the SNP mutation was introduced into Longjing 31 carrying the *Hap-T* haplotype, and the consequent substitution of thymine (T) with cytosine (C) at positions 34863184 and 34863187 on chromosome 1 yielded the *Hap-C* haplotype lines Longjing $31^{T\text{-}C}$-1 and Longjing $31^{T\text{-}C}$-2 (Supplementary Fig. S23). Compared with Longjing 31, Longjing $31^{T\text{-}C}$ only showed a slight decrease in the number of secondary branches per panicle and panicle length (Supplementary Table S6). Under both CLD

and CSD conditions, the heading dates of Longjing $31^{T\text{-}C}$-1 and Longjing $31^{T\text{-}C}$-2 were later than that of Longjing 31 (Fig. 6, B and C). To elucidate the mechanism underlying the earlier heading date of rice varieties carrying the *Hap-T* compared to that carrying the *Hap-C*, two types of promoters from the *OsWOX13*, designated as *OsWOX13-P1T* and *OsWOX13-P1C*, were constructed and employed as reporters (Fig. 6D). The relative LUC activity of promoter *OsWOX13-P1C* was significantly lower than that of promoter *OsWOX13-P1T* (Fig. 6E). EMSA demonstrated that Ehd1 bound more tightly to *P2-2-T* than to promoter *P2-2-C* (Fig. 6F). Subsequently, the expression levels of *OsWOX13* and *Hd3a* were determined in leaves of rice carrying the two haplotypes. The average expression levels of *OsWOX13* and *Hd3a* in leaves of rice carrying the *Hap-T* were significantly higher than those in rice carrying the *Hap-C* (Fig. 6, G to J). Meanwhile, the relative expression levels of *OsWOX13* and *Hd3a* in both Longjing $31^{T\text{-}C}$-1 and Longjing $31^{T\text{-}C}$-2 were significantly lower than those in Longjing 31 (Fig. 6, K to N). The SNP likely fine-tuned *OsWOX13* expression levels by partially attenuating Ehd1 binding and activation, and these results indicated that Ehd1 activated *OsWOX13* to a lesser extent in *Hap-C* than in *Hap-T*, thereby reducing *Hd3a* expression and consequently delaying heading date in rice.

Among *Hap-C* rice, *Indica* accounted for 88.5%, followed by varieties *Aus* and *Japonica*, each comprising 4.1% (Supplementary Fig. S24A). In contrast, among *Hap-T* rice, *Japonica* constituted 76.5%, followed by *Aus* and *Basmati*, which accounted for 11.9% and 5.9%, respectively, while *Indica* represented only 2.4% (Supplementary Fig. S24B). Furthermore, *Hap-C* accounted for 98.6% in *O. sativa Indica* (Supplementary Fig. S24C), whereas in *O. sativa Japonica*, *Hap-C* accounted for only 9.6% and *Hap-T* accounted for 90.4% (Supplementary Fig. S24D). However, in *O. rufipogon IIIa*, the wild ancestor of *O. sativa Japonica*, *Hap-T* accounted for 48.4% and *Hap-C* for 51.6% (Supplementary Fig. S24E). These results indicate that the *Hap-T* haplotype was subjected to artificial selection during rice domestication. Meanwhile, rice carrying the *Hap-T* was predominantly cultivated in high-latitude regions of Europe, whereas rice carrying the *Hap-C* was mainly grown in low-latitude regions of Africa, America, and Asia (Fig. 7A). Within Asia, rice with the *Hap-C* was primarily cultivated in low-latitude areas, while that with the *Hap-T* was more prevalent in high-latitude regions (Fig. 7B). These results indicated that rice carrying the *Hap-T*, which exhibited earlier heading, had been selectively

cultivated in high-latitude regions to adapt to the shorter growing seasons characteristic of these areas.

Discussion

The *Ehd1-Hd3a*/*RFT1* pathway mediates photoperiodic heading in rice, which is unique to this species (Cai et al. 2021). Numerous studies indicate that Ehd1 indirectly regulates the expression of *Hd3a*/*RFT1*, thereby modulating the heading date in rice (Doi et al. 2004; Matsubara et al. 2008; Itoh et al. 2010; Wei et al. 2010). Thus, the mechanism by which Ehd1 transmits the integrated heading signals to Hd3a through a particular protein and precisely regulates *Hd3a* expression remains unknown. In this study, we found that Ehd1 binds to the promoter of *OsWOX13* and activates its expression (Fig. 1). Moreover, Ehd1 more significantly upregulates the expression of *OsWOX13* in *Hap-T* than in *Hap-C* (Fig. 6, G to N). OsWOX13 can interact with the *Hd3a* promoter to enhance its expression, thereby regulating rice heading date (Fig. 3). Meanwhile, the interaction between OsWOX13 and Hd3a attenuates the promotion of *Hd3a* expression, that precisely modulates *Hd3a* levels and accurately regulates rice heading date (Fig. 4). Furthermore, genetic studies confirmed that *Ehd1* and *OsWOX13* coordinately regulated heading date in rice (Fig. 2), and the same regulatory relationship applies to *OsWOX13* and *Hd3a* (Fig. 5). Based on these findings, we propose a novel *Ehd1-OsWOX13-Hd3a* regulatory pathway for heading date (Fig. 8).

The rice *WOX* family consists of 13 members in total, which can be clearly divided into three evolutionary clades: the ancient clade, the intermediate clade, and the modern clade (Van et al. 2009). *OsWOX13* belongs to the ancient clade of the *WOX* family and is relatively conserved. This suggests potential functional divergence from other members (Deveaux et al. 2008). In this study, ChIP-Seq results showed that only the promoter of the *OsWOX13* among the *WOX* family members was enriched (Supplementary Table S2). Further, molecular and genetic evidence demonstrated that *OsWOX13* mediates the regulatory effect of Ehd1 on *Hd3a* expression, forming the *Ehd1-OsWOX13-Hd3a* regulatory pathway. Therefore, it is speculated that this pathway is a relatively specific pathway in the regulation of rice heading date. However, OsWOX13 only mediates part of the heading signal transmission in the *Ehd1-Hd3a* pathway. First, OsWOX13 does not regulate the expression of *Ehd1* (Supplementary Fig. S19). Second, compared with NIP, the expression levels of *Hd3a* showed a downward trend in the *Oswox13*,

but the expression level of *Hd3a* in the *Oswox13 ehd1* was further decreased compared with that in the *Oswox13*, which was consistent with that in the *ehd1* (Supplementary Fig. S20, A and B). Moreover, Ehd1 could still activate the expression of *Hd3a* in the *Oswox13*, with a stronger activation observed in Nip (Supplementary Fig. S20C). These results indicate that Ehd1 has a more powerful function in regulating heading date in rice, and *OsWOX13* is not the only downstream gene of *Ehd1*. This may be the reason why the heading date phenotype of the *Oswox13 ehd1* is consistent with that of the *ehd1* single mutant, without showing an additive effect.

Hd3a and *RFT1*, as downstream genes of Ehd1, appear to be regulated by Ehd1 through distinct mechanisms. The transcription of *Hd3a* was found to be entirely dependent on functional Ehd1, while *RFT1* expression was regulated by both Ehd1 and additional mechanisms (Zhao et al. 2015). SET domain group protein 724 (SDG724) specifically affects the histone H3-lysine36me2/3 levels at the *RFT1* locus but not its close paralog *Hd3a* (Sun et al. 2012). Se14 regulated chromatin structure through H3K4me3 demethylation in the promoter region of *RFT1*, thereby regulating heading date (Yokoo et al. 2014). Under LD conditions exceeding 13.5 hours, the expression of *Hd3a* declines significantly, whereas *RFT1* expression remains relatively stable (Itoh et al. 2010). Meanwhile, the homology between the promoter sequences of *Hd3a* and *RFT1* was also very low, at only 20.51% (Supplementary Fig. S25). Furthermore, although *Hd3a* was genetically confirmed as the downstream target of *OsWOX13* in regulating heading date (Fig. 5), *OsWOX13* is still able to modulate *RFT1* expression (Kim. 2024). However, the expression level of *RFT1* was unchanged in *OsWOX13-OE hd3a* and *hd3a* (Supplementary Fig. S26), and no OsWOX13-binding motif was identified in the *RFT1* promoter. These findings suggest that OsWOX13 may regulate *RFT1* expression in an *Hd3a*-dependent manner. Flowering activating complexes (FACs) were found to form in leaves, where Hd3a and RFT1 interacted with OsFD1 via Gf14c (Brambilla et al. 2017). These complexes were essential for activating a positive feedback loop in the expression of *Ehd1*, *Hd3a*, and *RFT1*. This may account for the regulatory effect of *Hd3a* on *RFT1* expression. In conclusion, these findings collectively demonstrate that Ehd1, which integrates multiple heading signals, transmitted them separately to *Hd3a* and *RFT1*. *OsWOX13* was not the sole downstream target of *Ehd1* in this process. The specific proteins through which Ehd1 transmitted the heading signal to *RFT1* remained to be further investigated.

In *Arabidopsis thaliana*, the *FLOWERING LOCUS T* (*FT*) gene has been identified as the ultimate regulator of flowering (Bai et al. 2024). In rice, *Hd3a* and *RFT1* have been identified as orthologs of the *Arabidopsis FT* and have been found to be crucial for rice heading (Komiya et al. 2008; Tsuji et al. 2010). Thus, the accurate expression levels of florigen genes are crucial for heading in plants. The Arabidopsis DWARF14 responded to strigolactones by stabilizing TARGET OF EAT1 (TOE1) to suppress *FT* transcription and by degrading SUPPRESSOR OF MAX2-LIKE 7 to enhance TOE1-mediated repression of the *FT* promoter, thereby precisely regulating *FT* expression and accurately controlling flowering in Arabidopsis (Bai et al. 2024). In rice, the expression of *Hd3a* and *RFT1* was indirectly regulated via two pathways, the Ehd1 and Hd1 pathways (Li et al. 2022). In this study, Ehd1, which integrates multiple heading signals, promoted the expression of *OsWOX13* (Fig. 1). OsWOX13 directly bound to the *Hd3a* promoter to enhance its expression (Fig. 3), while also interacting with the Hd3a protein to inhibit OsWOX13-mediated activation of *Hd3a* expression (Fig. 4). We speculate that the interaction between Hd3a and OsWOX13 represses the transcriptional activation of *Hd3a* by OsWOX13 through possible dual mechanism: on one hand, this interaction inhibits the transcriptional activity of OsWOX13 (Supplementary Fig. S21); on the other hand, it may spatially interfere with the DNA-binding ability of OsWOX13 (Fig. 4E). Our study revealed a regulatory mechanism involving OsWOX13 that maintains *Hd3a* expression levels, thereby precisely regulating the heading date in rice (Fig. 8). Since the accumulation of Hd3a protein repressed further activation by OsWOX13 on *Hd3a*, this may explain the weakened activation of *Hd3a* expression by OsWOX13 at night (Fig. 3). We also do not rule out the possibility that other genes are involved in this regulatory process. Future research should focus on identifying additional proteins that precisely regulate the expression of the florigen genes *RFT1* to further refine the heading date regulatory network, thereby enabling more accurate control of rice heading.

In rice, the heading date is an important agronomic trait for climatic and regional adaptability (Sun et al. 2012). Therefore, the exploration of haplotypes for heading date-regulating genes and the dissection of their regulatory mechanisms are of substantial significance for enhancing the regional adaptability of rice varieties. In our study, we characterized a SNP within the *P2-2* region of the *OsWOX13* promoter, which segregated into two haplotypes: *Hap-T* and *Hap-C*. Rice varieties carrying the *Hap-T* exhibited earlier heading compared to those with

the *Hap-C* (Fig. 6A to C). We further predicted the chromatin accessibility of the region harboring this SNP and found that it exhibited a high accessibility score of 91%, indicating a highly open regulatory region. Meanwhile, this phenotypic difference was associated with the capacity of *Ehd1* to enhance the expression of *OsWOX13* and *Hd3a* more effectively in the *Hap-T* (Fig. 6, G to N). We therefore speculate that this SNP may reduce the chromatin accessibility of this region, thereby weakening the binding efficiency of Ehd1 to this locus. Although we generated the Longjing $31^{T\text{-}C}$ lines carrying *Hap-C* in the Longjing 31 background, and these lines exhibited later heading date than Longjing 31, genetically and molecularly validating that this SNP regulates rice heading date, we cannot rule out the possibility that the overall earlier heading of the *Hap-T* compared with the *Hap-C* in the natural population is partly attributable to population structure differences between *Japonica* and *Indica*. Furthermore, in *O. rufipogon IIIa* (the wild ancestor of *O. sativa Japonica*), *Hap-T* accounted for 48.4% and *Hap-C* for 51.6% (Supplementary Fig. S24E). By contrast, in cultivated *O. sativa Japonica*, the frequency of *Hap-C* dropped to only 9.6%, while *Hap-T* increased to 90.4% (Supplementary Fig. S24D). Meanwhile, rice varieties harboring the *Hap-T* were predominantly cultivated in high-latitude regions to adapt to the shorter growing seasons (Fig. 7). These results indicate that the *Hap-T* haplotype was subjected to artificial selection during rice domestication. As reported in previous studies, the *Hd3a-435G* allele enables rice to head 10 days earlier under NLD conditions in high-latitude regions (Han et al. 2023). Additionally, the frequency of the *Hd3a-435G* allele increased from low to high latitudes, thereby facilitating the improvement of regional adaptability in rice. Genetic variations in the promoters of *OsWOX13* enabled fine-tuning of rice heading date, thereby facilitating adaptation to diverse cultivation regions. For example, the editing of the *Hd1* promoter led to early heading in rice, facilitating its cultivation in high-latitude regions (Zhou et al. 2024). These results indicate that our study provides valuable genetic resources for improving the regional and climatic adaptability of rice.

Methods

Plant materials and growth conditions

The genome sequence of the *Japonica* rice cultivar Nip has been sequenced to a high-quality level (Matsumoto et al. 2016). Thus, the Nip was chosen as the genetic background material for the construction of mutants and gene overexpression (OE) lines. All rice materials

were planted in Beijing (NLD, 40°13′N, 116°13′E) and Hainan (NSD, 18°48′N, 110°02′E). Meanwhile, rice materials were also grown in light incubators under controlled long day (CLD, 14 h light 30℃/10 h dark 25℃) or control short day (CSD, 10 h light 30℃/14 h dark 25℃), with a light intensity of 500-800 μmol·m^{-2}·s^{-1} and relative humidity of 70%. Under the same growth conditions, all rice materials were cultivated using identical management practices.

Vector and genetic material constructions

The coding sequences of *Ehd1*, *OsWOX13* and *Hd3a* were cloned from rice leaves and were fused to various vectors. We generated *Pro35S:*OsWOX13-FLAG and *ProUbi:*OsWOX13 (Supplementary Table S7). Meanwhile, 18- or 20-bp gene-specific spacer sequences targeting *Ehd1*, *OsWOX13* and *Hd3a* were cloned into the sgRNA/Cas9 vector. Further, the above constructs were introduced into *Agrobacterium tumefaciens* (EHA105) and then transformed into the callus of Nip. Then, we obtained *OsWOX13-OE-1*, *-2*, *-3*, *-4*, *ehd1-2*, *Oswox13-1*, *-2*, *-3* genetic materials. The *ehd1-1* and *hd3a-1* mutants were previously generated (Zhu et al. 2017; Chai et al. 2021).

To generate *Oswox13 ehd1* and *Oswox13 hd3a* double mutants and *OsWOX13-OE hd3a* lines, we utilized *ehd1-1*, *ehd1-2*, *hd3a-1* as the recipient materials for genetic transformation, respectively, and targeted the knockout and overexpression of the *OsWOX13* gene. Further, we generated the double mutant *Oswox13-2 hd3a-2* by simultaneously knocking out *OsWOX13* and *Hd3a* in the NIP background.

To ensure the accuracy of the ChIP-qPCR assay, *ProEhd1:Ehd1-GFP* was introduced into material *ehd1-2*, and *ProOsWOX13: OsWOX13-FLAG* was introduced into material *Oswox13-2*, thereby generating materials *ProEhd1:Ehd1-GFP ehd1-2* and *ProOsWOX13: OsWOX13-FLAG Oswox13-2*, respectively.

To characterize the genetic regulation of a SNP within the *OsWOX13* promoter (Chr 1: 34863184) on rice heading date, a target-specific sgRNA (sgRNA-OsA1) was designed to precisely edit this SNP locus (Supplementary Table S7). No other potential off-target sites were identified through online prediction (https://www.rgenome.net/cas-offinder/). The sgRNA-OsA1 fragment was then cloned into vector pH-CP-ABE8e-RY^{KK} via recombinant technology, and the resulting recombinant vector was subsequently transformed into the rice cultivar Longjing 31.

Both thymine (T) residues at positions 34863184 and 34863187 on chromosome 1 were simultaneously mutated to cytosine (C), generating two lines (Longjing $31^{T\text{-}C}$-1 and Longjing $31^{T\text{-}C}$-2) from independent separate transgenic events.

To generate transgene homozygous lines, we first identified the expression levels of *Ehd1* and *OsWOX13* in the overexpressing lines using real-time polymerase chain reaction (qRT-PCR) (Supplementary Table S7). Subsequently, the total protein was extracted from the leaves of these transgenic lines. Western blot analysis was then performed to detect the expression of the corresponding labeled proteins. Meanwhile, the mutant materials were identified by sequencing. All transgenic lines used in this study were derived from distinct primary transformants, identified and advanced to homozygous T_2-T_5 generations, and subjected to phenotypic observations and biochemical assays.

Measurement of agronomic traits

We conducted a comprehensive investigation of the agronomic traits of all plants that were grown in Beijing, except for Longjing 31 which was cultivated under CSD conditions. The traits examined included plant height, panicle length, number of primary branches/panicle, number of secondary branches/panicle, grain number/panicle, tiller number, 1000-grain weight and setting rate/panicle. Meanwhile, the heading time of all genetic materials grown in Beijing, Hainan, CSD and CLD was investigated. For each agronomic trait, a comprehensive investigation was conducted on 20 plants for each line.

RNA extraction and qRT-PCR analyses

To investigate the expression patterns of *OsWOX13* and *Hd3a* genes within a 48-hour period, RNA was extracted from rice leaves grown under CSD conditions for 25 days and from those grown in Beijing for 65 days. At the same rice growth stage, the expression levels of *RFT1*, *Ehd1* and *Hd3a* were determined in different lines at 4 h after dawn. Meanwhile, we also extracted RNA from different tissues of Nip to assess the expression patterns of *Ehd1*, *OsWOX13* and *Hd3a*.

Forty rice varieties each with the *Hap-T* or *Hap-C* haplotype were randomly selected, followed by growth under CSD for 25 days or CLD for 50 days (Supplementary Table S8). In

parallel, Longjing 31, Longjing $31^{T\text{-}C}$-1 and Longjing $31^{T\text{-}C}$-2 were cultivated under CSD for 35 days or CLD for 45 days. Subsequently, RNA was extracted from the leaf samples of all groups.

Further, total RNA was extracted from protoplasts of NIP, as well as from the *Oswox13* and NIP overexpressing *Ehd1*, and the *Oswox13* without *Ehd1* overexpression. qRT-PCR primers were designed in the 3' UTR region of *Hd3a* to identify the relative expression level of endogenous *Hd3a*.

Total RNA was extracted using a Quick-RNA™ Plant Miniprep Kit (ZYMO RESEARCH, America). The RNA was reverse-transcribed using a FastKing RT Kit (Tiangen, China). According to the TB Green Premix Ex Taq™ II FAST qPCR kit instructions (TaKaRa, Japan), the qRT-PCR was performed. The expression level of gene was assessed using *gene*/*UBQ* or $2^{-\Delta\Delta CT}$ method. The rice *Ubiquitin* (*UBQ*) gene was used as an internal control. Significance was assessed using a two-tailed Student's *t*-test or using ANOVA followed by Tukey's test ($P<0.05$). In this study, the primers used are listed in Supplementary Table S7.

RNA in situ hybridization

The experimental procedure for RNA in situ hybridization was performed as described previously (Zhang et al. 2025). Leaves of NIP grown for 25, 30, and 35 days were sampled, fixed in FAA fixative, subjected to gradient dehydration and transparency treatment followed by paraffin embedding, and then sectioned into 10 μm-thick slices. Gene-specific probes were designed for *Ehd1*, *OsWOX13* and *Hd3a*, respectively; the antisense probes were used as the experimental group for gene expression detection, while the sense probes served as the negative control to eliminate non-specific signals. Specifically, the *OsWOX13* probe was labeled with fluorescence (Roche, 11685619910), whereas the *Ehd1* and *Hd3a* probes were labeled with DIG. RNA in situ hybridization was performed on leaf sections using the prepared mixed probes. After hybridization, the slides were first incubated with fluorescence-labeled antibodies (Roche, 11426338910) and stained with Fast Red. The antibodies were then eluted, followed by incubation with digoxigenin-labeled antibodies (Roche, 11093274910) and subsequent chromogenic reaction with NBT solution. Stem of NIP grown for 40, 45, and 50 days were sampled and subjected only to NBT staining, following the same procedure as described above.

ChIP sequence and qPCR assay

The ChIP assay was performed as previously described (Duan et al. 2019). ChIP-Seq was performed on leaves of the *Ehd-OE-1* line grown for 80 days, and its binding motifs were analyzed. ChIP-seq sequencing was performed on the Illumina NovaSeqTM X Plus platform with two biological replicates for each sample, and the sequencing depth was 6 G per sample. The FLAG antibody used in this study was purchased from Sigma (F1804). Peak calling was conducted using MACS2 software, and the threshold for peak filtering was set at a q-value < 0.05. Raw peak files of ChIP-Seq data are presented in Supplementary Data set 1. Motif enrichment analysis was performed using HOMER based on the full sequences of individual peaks, with a cutoff threshold of $P < 0.01$. The leaves of the *Ehd1-OE-1*, *ProEhd1:Ehd1-GFP ehd1-2*, *OsWOX13-OE-1* and *ProOsWOX13:OsWOX13-FLAG Oswox13-2*, lines at 80 days of age were subjected to formaldehyde cross-linking. Meanwhile, *ProOsWOX13:OsWOX13-FLAG* was transformed into rice protoplasts generated from Nip and *hd3a-1* were subjected to formaldehyde cross-linking. Subsequently, leaves were collected for sequencing (IGENEBOOK, China). Meanwhile, leaves chromatin was extracted and fragmented using ultrasonication to an average size of approximately 200-500 bp. The protein A magnetic beads (Merck Milli-pore, 16-661), anti-DDDDK-tag mab (MBL, M185-3L) and anti-GFP antibody (Roche, 11814460001) were used for immunoprecipitation. Finally, the purified DNA was a template for the qPCR. The ratio of IP to input and fold enrichment was used as the result of enrichment. *Actin* was used as a negative control. In this assay, the primers used are listed in Supplementary Table S7.

Transcriptome sequence

The NIP, *OsWOX13-OE-1* and *Oswox13-2* were grown in Beijing for 80 days, and their leaves were harvested at 4 h after dawn. and sent to Majorbio for transcriptome sequencing. KEGG enrichment analysis was performed using the union of differentially expressed genes from NIP, *OsWOX13-OE-1* and *Oswox13-2*. The KEGG enrichment pathways shown in the figure are based on a significance threshold of $P<0.1$.

Protein expression and purification

To generate GST and His-tag fusion proteins, the full-length coding sequences of *Ehd1*, *OsWOX13*, and *Hd3a* were cloned. The *Ehd1* and *Hd3a* sequence was then inserted into the pGEX-4T-2 vector, while *OsWOX13* and *Hd3a* were inserted into the pET-30a vector. The proteins His, GST, GST-Ehd1, GST- Hd3a, His, His-OsWOX13, and His-Hd3a were expressed

in *E. coli* strain DE3. They were subsequently solubilized in PBS buffer containing 1 mM DTT and a 1× protease inhibitor cocktail, captured using GST- or His-tagged beads (Beaver Biosciences Inc, China), and eluted with 20 mM glutathione or 200 mM imidazole, respectively.

EMSA

Conduct EMSA assays following the LightShift® Chemiluminescent EMSA Kit protocol (Thermo Fisher Scientific, America). The 5' biotin-labeled probes used in this experiment were synthesized (Sangon Biotech, China)(Supplementary Table S7), the competitors were probes that were not labeled with biotin, and subsequently annealed into double-stranded structures (Zhang et al. 2025).

LUC activity determination

The promoter region (*OsWOX13-P1*) of *OsWOX13* (2000 bp upstream of the ATG start codon, the ATG, and a 69 bp downstream fragment identified by ChIP-Seq), *OsWOX13-P2* and its sub-fragments was fused into the pGreen0800-LUC vector as a reporter. The 2000-bp *OsWOX13* promoter (*OsWOX13-P1T*), the 2500-bp *Hd3a* promoter (*Hd3a-P1*) and *Hd3a-P2* were inserted into the pGreen0800-LUC vector as reporters. The 54th base T upstream of the ATG start codon in construct *OsWOX13-P1T* was mutated to C and then fused into the vector, resulting in construct *OsWOX13-P1C*. The *Ehd1* and *OsWOX13* genes were subsequently introduced into the pPAN580-FLAG vector as effectors. The pPAN580-FLAG vector without any genes was used as a control. Effector and reporter constructs were co-transformed into rice protoplasts. Hsp82 was used as an internal reference protein.

OsWOX13, OsWOX13$^{1\text{-}90\ aa}$, OsWOX13$^{90\text{-}150\ aa}$ and OsWOX13$^{151\text{-}268\ aa}$ were individually fused with Gal4BD, and then co-transformed with either *UAS*, GFP or Hd3a-GFP into rice protoplasts isolated from *hd3a* mutant. Gal4BD empty vector was used as the negative control, and VP16-Gal4BD as the positive control. Rice protoplast preparation and the transient expression assay were performed as previously described (Zhang et al. 2011). After 16 h, proteins were extracted protein extraction buffer (50 mM Tris-HCl, pH 8.0, 1 mM $MgCl_2$, 10 mM EDTA, 0.5 M sucrose, 5 mM DTT, 0.3% [v/v] triton X-100 and 1× protease inhibitor) and the LUC assay was performed as per the Double-Luciferase Assay Kit (Promega) protocol. The relative LUC activity was calculated as the ratio of LUC/REN.

Yeast two-hybrid assays

Yeast two-hybrid assays were performed as previously described (Zhang et al. 2025). The coding region of *Hd3a* was cloned into pGADT7 (prey). OsWOX13, OsWOX13$^{1\text{-}90\ aa}$, OsWOX13$^{90\text{-}150\ aa}$ and OsWOX13$^{151\text{-}268\ aa}$ into pGBKT7 (bait). Bait and prey constructs were co-transformed into yeast AH109, selected on SD/-Leu-Trp medium, and their interaction was tested on SD/-Leu/-Trp/-His/-Ade medium at 30 °C for 3 d.

Firefly LUC complementation imaging assays

Split-LUC assays were performed as previously described (Zhang et al. 2025). The OsICE2, OsWOX13$^{1\text{-}90\ aa}$ and OsWOX13$^{151\text{-}268\ aa}$ were cloned into the pCAMBIA-nLUC vector, as well as OsICE2 and Hd3a were inserted into the pCAMBIA-cLUC vector. All recombinant constructs were transformed into Agrobacterium tumefaciens EHA105 and infiltrated into *Nicotiana benthamiana* leaves. After 48 h, leaves were treated with 1 mM luciferin for 5 min, and LUC activity was detected using a NightShade LB 985 imaging system.

Subcellular localization and bimolecular fluorescence complementation

The *OsWOX13* gene coding sequence was cloned into a pAN580-GFP vector and introduced into rice protoplasts, followed by fluorescence observation using confocal microscopy (LSM 980, Zeiss). D53-mCherry was used as a nucleus marker.

The coding sequences of *OsICE2*, *OsWOX13* and *Hd3a* were cloned into vectors pSPYNE173 and pSPYCE173, respectively, and introduced into *Agrobacterium tumefaciens* strain EHA105. D53-mCherry was used as a nucleus marker. *N. benthamiana* leaves were infected with *Agrobacterium tumefacien* (Waadt and Kudla 2008), and fluorescence signals were detected by confocal microscopy 48 hours post-infection. Random fields of view were selected for imaging to acquire subcellular localization and BiFC data, and a total of 10 independent fields were observed.

Western blot

The proteins were boiled at 95°C for 10 min with SDS-PAGE loading buffer (CWBio, China). Proteins were separated in 10% SDS-PAGE gels and detected with anti-DDDDK-tag mab (MBL, M185-3L, 1:5000), anti-GFP antibody (Roche, 11814460001, 1:5000), anti-GST

antibodies (Medical Biological Laboratories, PM013-7, 1:5000) and anti-His antibodies (Medical Biological Laboratories, D291-7, 1:5000), anti-HSP82 (AbM51099-31-PU, 1:5000) respectively. Some primary antibodies require incubation with secondary anti-IgG antibody (MBL, 330, 1:5000). Finally, the ECL reagent from Bio-Rad was used for immunoblot testing.

In vivo Co-IP assay

The coding sequences of *OsWOX13* and *Hd3a* were cloned into vectors pCAMBIA1300 (containing a FLAG tag) and pCAMBIA1305 (containing a GFP tag), respectively, and introduced into *Agrobacterium tumefaciens* strain EHA105. *N. benthamiana* leaves were infected with *Agrobacterium tumefaciens*, and total protein were extracted by protein extraction buffer at 48 hours post-infection. The 80 μL of total protein was retained as input, and the remaining proteins were incubated with anti-FLAG-tag mAb-magnetic agarose (M185-10R, MBL) at 4°C for 1 h. The subsequent procedures were adapted from prior studies and included western blot analysis (Zhang et al. 2025).

In vitro pull-down assay

The GST, GST- Hd3a and His-OsWOX13 were expressed in *E. coli* strain DE3. They were subsequently resuspended in TBS buffer (25 mM Tris–HCl [pH 7.5], 50 mM NaCl, 1 mM DTT, and 1×protease inhibitor cocktail). Equal amounts of GST and GST-Hd3a were each mixed with His and His-OsWOX13 protein. A total of 80 μL of the protein mixture was retained as input, and the remaining mixture was incubated with His-tagged beads at 4°C for 3 hours. The subsequent procedures were adapted from prior studies and included western blot analysis (Cai et al. 2021).

Analysis of haplotype-heading date correlation and geographic distribution.

The allelic variation of the *OsWOX13* gene was assessed using a rice functional genomics and breeding database version 2.0 (https://v1.rmbreeding.cn) (Wang et al. 2018). The *OsWOX13* gene was classified into two haplotypes (*Hap-T* and *Hap-C*) based on an SNP at position 34863184 on chromosome 1. The chromatin accessibility at this locus was also predicted using RiceVarMap v2.0 (http://ricevarmap.ncpgr.cn/v2/). Meanwhile, the distribution proportion of *Hap-T* and *Hap-C* in different subspecies was analyzed based on previous data (Guo et al. 2025).

Subsequently, the geographical coordinates (longitude and latitude) of the capital cities of the countries of origin for the rice varieties in the database, as well as those of the diverse rice cultivation regions in China, were obtained. The global and Asian geographic distribution of the two haplotypes of rice varieties was visualized.

Statistical analysis

All experiments were conducted with three biological replicates. The statistical results are presented as means ± SD, with n denoting the number of biological replicates. Three separate plants per tissue sample were combined to form three biological replicates in qRT-PCR analysis. Significance was assessed using a two-tailed Student's *t*-test or using ANOVA followed by Tukey's test ($P<0.05$). Different lowercase letters in the figure indicate significant differences between groups based on Tukey's comparisons. The statistical methods used for each experiment were detailed in the Supplementary Date set 2.

Phylogenetic tree

Homologous family proteins were screened using the domain, and a neighbor-joining phylogenetic tree was constructed with MEGA 7.0 with 1000 bootstrap replicates, based on full-length amino acid sequences from rice. The sequence alignment files and phylogenetic tree files for LOC_Os01g13090, LOC_Os02g46860, LOC_Os03g61200, LOC_Os06g08350 and LOC_Os12g01410 were presented as Supplementary Data set 3-7 and Supplementary Data set 8-12, respectively.

The information of antibodies

Digoxigenin-labeled antibodies (Roche, 11093274910), Fluorescence-labeled antibodies (Roche, 11426338910), FLAG antibody Sigma (F1804), Anti-DDDDK-tag mab (MBL, M185-3L), Anti-GFP antibody (Roche, 11814460001), Anti-GST antibodies (Medical Biological Laboratories, PM013-7), Anti-His antibodies (Medical Biological Laboratories, D291-7), Anti-HSP82 (AbM51099-31-PU), Antibody-lgG (H + L chain) Mouse pAb-HRP (MBL, Code No: 330).

Accession numbers

The sequences of the genes related to this study are available on the Rice Genome Annotation Project and the *Arabidopsis* TAIR database under the following accession numbers:*Ehd1* (*LOC_Os10g32600*), *OsWOX13* (*LOC_Os01g60270*), *Hd3a* (*LOC_Os06g06320*), *OsFTL12* (*LOC_Os06g35940*), *OsELF3.2* (*LOC_Os01g38530*), *OsPHYA-like* (*Os03g0719700*), *RFT1* (*LOC_Os06g06300*), *OsICE2* (*LOC_Os01g70310*), *DHD4* (*LOC_Os02g01990*), *SDG724* (*LOC_Os09g13740*), *Se14* (*LOC_Os03g05680*), *OsFD1* (*LOC_Os09g36910*), *FT* (*At1g65480*), *AtD14* (*AT3g03990*), *TOE1* (*At2g28550*), *SMXL7* (*AT2g29970*).

ChIP-Seq and transcriptome data generated in this study have been deposited in the NCBI database, with the corresponding accession numbers as follows: *SRP698665* and *SRP693703*.

Acknowledgements

We extend our sincere gratitude to Xinhao Ouyang from Xiamen University for providing the seeds of the Ehd1 overexpression lines in the NIP background. We also express our sincere thanks to Yu Zhao from Huazhong Agricultural University for supplying the *Oswox13* mutant in the ZH11 background.

Author contributions

J.W. and S. Z. supervised the project and designed the research. S. Z. and M. Y. wrote the paper. M. Y. performed most of the experiments. M. Y. and M. C. analyzed the data. M. C. performed RNA in situ hybridization. X.Z. conducted the related protoplast assays. M. C., X. Z., M. W., L. Z., W. L., X. J., L. M., and Q. Y. cultivated the transgenic plants in the field. Y. L. and B. L. analyzed the geographical distribution of the *OsWOX13* haplotypes.

Funding

This work was supported by the Agriculture Science and Technology Major Project, the Innovation Program of Chinese Academy of Agricultural Sciences (Y2026YC02), the State Key Laboratory of Crop Gene Resources and Breeding (S2026QZ13) and the Inner Mongolia Innovation Center of Biological Breeding Technology.

Competing interests

All authors have approved the manuscript and declare no conflicts of interest.

Data availability

The data underlying this article are available in the article and in its online supplementary material.

References

Bai JR, Lei X, Liu JL, Huang Y, Bi LM, Wang YH, Li JD, Yu HY, Yao SX, Chen L, et al. The strigolactone receptor DWARF14 regulates flowering time in Arabidopsis. Plant Cell. 2024: 36(11): 4752–4767. https://doi.org/10.1093/plcell/koae248

Brambilla V, Fornara F. Molecular control of flowering in response to day length in rice. J Integr Plant Biol. 2013: 55(5): 410–418. https://doi.org/10.1111/jipb.12033

Brambilla V, Martignago D, Goretti D, Cerise M, Somssich M, de Rosa M, Galbiati F, Shrestha R, Lazzaro F, Simon R, et al. Antagonistic transcription factor complexes modulate the floral transition in rice. Plant Cell. 2017: 29(11): 2801–2816. https://doi.org/10.1105/tpc.17.00645

Cui YX, Wang JR, Feng L, Liu S, Li JQ, Qiao WH, Song Y, Zhang ZQ, Cheng YL, Zhang LF, et al. A combination of long-day suppressor genes contributes to the northward expansion of rice. Front Plant Sci. 2020: 11: 864. https://doi.org/10.3389/fpls.2020.00864

Cai MH, Zhu SS, Wu MM, Zheng XM, Wang JC, Zhou L, Zheng TH, Cui S, Zhou SR, Li CN, et al. DHD4, a CONSTANS-like family transcription factor, delays heading date by affecting the formation of the FAC complex in rice. Mol Plant. 2021: 14(2): 330–343. https://doi.org/10.1016/j.molp.2020.11.013

Chai JT, Zhu SS, Li CN, Wang CM, Cai MH, Zheng XM, Liang Z, Zhang H, Sheng PK, Wu MM, et al. OsRE1 interacts with OsRIP1 to regulate rice heading date by finely modulating Ehd1 expression. Plant Biotechnol J. 2021: 19(2): 300–310. https://doi.org/10.1111/pbi.13462

Chen JY, Zhang HW, Zhang HL, Ying JZ, Ma LY, Zhuang JY. Natural variation at qHd1 affects heading date acceleration at high temperatures with pleiotropism for yield traits in rice. BMC Plant Biol. 2018: 18(1): 112. https://doi.org/10.1186/s12870-018-1330-5

Deveaux Y, Toffano-Nioche C, Claisse G, Thareau V, Morin H, Laufs P, Moreau H, Kreis M, Lecharny A. Genes of the most conserved *WOX* clade in plants affect root and flower development in Arabidopsis. BMC Evol Biol. 2008: 8: 291. https://doi.org/10.1186/1471-2148-8-291

Doi K, Izawa T, Fuse T, Yamanouchi U, Kubo T, Shimatani Z, Yano M, Yoshimura A. Ehd1, a B-type response regulator in rice, confers short-day promotion of flowering and controls *FT-like* gene expression independently of Hd1. Genes Dev. 2004: 18(8): 926–936. https://doi.org/10.1101/gad.1189604

Duan EC, Wang YH, Li XH, Lin QB, Zhang T, Wang YP, Zhou CL, Zhang H, Jiang L, Wang JL, et al. OsSHI1 regulates plant architecture through modulating the transcriptional activity of IPA1 in Rice. Plant Cell. 2019: 31(5): 1026–1042. https://doi.org/10.1105/tpc.19.00023

Gao H, Jin MN, Zheng XM, Chen J, Yuan DY, Xin YY, Wang MQ, Huang DY, Zhang Z, Zhou KN, et al. Days to heading 7, a major quantitative locus determining photoperiod sensitivity and regional adaptation in rice. Proc Natl Acad Sci U S A. 2014: 111(46): 16337–16342. https://doi.org/10.1073/pnas.1418204111

Gao H, Zheng XM, Fei GL, Chen J, Jin MN, Ren YL, Wu WX, Zhou KN, Sheng PK, Zhou F, et al. Ehd4 encodes a novel and Oryza-genus-specific regulator of photoperiodic flowering in rice. PLoS Genet. 2013: 9(2): e1003281. https://doi.org/10.1371/journal.pgen.1003281

Geng LP, Tan MF, Deng QY, Wang YJ, Zhang T, Hu XS, Ye MM, Lian XM. Zhou DX, Zhao Y. Transcription factors *WOX11* and *LBD16* function with histone demethylase JMJ706 to control crown root development in rice. Plant Cell. 2024: 36(5): 1777–1790. https://doi.org/10.1093/plcell/koad318

Guo DL, Li Y, Lu HY, Zhao Y, Kurata N, Wei XH, Wang AH, Wang YC, Zhan QL, Fan DL, et al. A pangenome reference of wild and cultivated rice. Nature. 2025: 642(8068): 662–671. https://doi.org/10.1038/s41586-025-08883-6

Han N, Tang R, Chen XQ, Xu ZX, Ren ZH, Wang LN. Genome-wide identification and characterization of *WOX* genes in *Cucumis sativus*. Genome. 2021: 64(8): 761–776. https://doi.org/10.1139/gen-2020-0029

Han ZM, Lei XL, Sha HJ, Liu J, Zhang CZ, Wang JG, Zheng HL, Zou DT, Fang J. Adaptation to high latitudes through a novel allele of *Hd3a* strongly promoting heading date in rice. Theor Appl Genet. 2023: 136(6): 141. https://doi.org/10.1007/s00122-023-04391-1

Hori K, Ogiso-Tanaka E, Matsubara K, Yamanouchi U, Ebana K, Yano M. *Hd16*, a gene for casein kinase I, is involved in the control of rice flowering time by modulating the day-length response. Plant J. 2013: 76(1): 36–46. https://doi.org/10.1111/tpj.12268

Huang XH, Yang SH, Gong JY, Zhao Q, Feng Q, Zhan QL, Zhao Y, Li WJ, Cheng BY, Xia JH, et al. Genomic architecture of heterosis for yield traits in rice. Nature. 2016: 537(7622): 629–633. https://doi.org/10.1038/nature19760

Huang XH, Zhao Y, Wei XH, Li CY, Wang A, Zhao Q, Li WJ, Guo YL, Deng LW, Zhu CR, et al. Genome-wide association study of flowering time and grain yield traits in a worldwide collection of rice germplasm. Nat Genet. 2011: 44(1): 32–39. https://doi.org/10.1038/ng.1018

Itoh H, Nonoue Y, Yano M, Izawa T. A pair of floral regulators sets critical day length for Hd3a florigen expression in rice. Nat Genet. 2010: 42(7): 635–638. https://doi.org/10.1038/ng.606

Jung C, Müller AE. Flowering time control and applications in plant breeding. Trends Plant Sci. 2009: 14(10): 563–573. https://doi.org/10.1016/j.tplants.2009.07.005

Kawai T, Shibata K, Akahoshi R, Nishiuchi S, Takahashi H, Nakazono M, Kojima T, Nosaka-Takahashi M, Sato Y, Toyoda A. *WUSCHEL-related homeobox* family genes in rice control lateral root primordium size. Proc Natl Acad Sci U S A. 2022: 119(1): e2101846119. https://doi.org/10.1073/pnas.2101846119

Kim SL, Lee S, Kim HJ, Nam HG, An G. OsMADS51 is a short-day flowering promoter that functions upstream of *Ehd1*, *OsMADS14*, and *Hd3a*. Plant Physiol. 2007: 145(4): 1484–1494. https://doi.org/10.1104/pp.107.103291

Kim YK. Knockout of *OsWOX13* moderately delays flowering in rice under natural long-day conditions. Biosci Biotechnol Biochem. 2024: 88(11): 1307–1315. https://doi.org/10.1093/bbb/zbae115

Komiya R, Ikegami A, Tamaki S, Yokoi S, Shimamoto K. Hd3a and RFT1 are essential for flowering in rice. Development. 2008: 135(4): 767–774. https://doi.org/10.1242/dev.008631

Lee YS, Jeong DH, Lee DY, Yi J, Ryu CH, Kim SL, Jeong HJ, Chop SC, Jin P, Yang J, et al. *OsCOL4* is a constitutive flowering repressor upstream of *Ehd1* and downstream of *OsphyB*. Plant J. 2010: 63(1): 18–30. https://doi.org/10.1111/j.1365-313X.2010.04226.x

Lian GB, Ding ZW, Wang Q, Zhang DB, Xu J. Origins and evolution of WUSCHEL-related homeobox protein family in plant kingdom. Sci World J. 2014: 2014: 534140. https://doi.org/10.1155/2014/534140

Li XF, Tian XJ, He ML, Liu XX, Li ZY, Tang JQ, Mei EY, Xu M, Liu YX, Wang ZY, et al. bZIP71 delays flowering by suppressing Ehd1 expression in rice. J Integr Plant Biol. 2022: 64(7): 1352–1363. https://doi.org/10.1111/jipb.13275

Matsubara K, Ogiso-Tanaka E, Hori K, Ebana K, Ando T, Yano M. Natural variation in Hd17, a homolog of Arabidopsis ELF3 that is involved in rice photoperiodic flowering. Plant Cell Physiol. 2012: 53(4): 709–716. https://doi.org/10.1093/pcp/pcs028

Matsubara K, Yamanouchi U, Wang ZX, Minobe Y, Izawa T, Yano M. *Ehd2*, a rice ortholog of the maize INDETERMINATE1 gene, promotes flowering by up-regulating *Ehd1*. Plant Physiol. 2008: 148(3): 1425–1435. https://doi.org/10.1104/pp.108.125542

Mukherjee K, Brocchieri L, Bürglin TR. A comprehensive classification and evolutionary analysis of plant homeobox genes. Mol Biol Evol. 2009: 26(12): 2775–2794. https://doi.org/10.1093/molbev/msp201

Matsumoto T, Wu JZ, Itoh T, Numa H, Antonio B, Sasaki T. The Nipponbare genome and the next-generation of rice genomics research in Japan. Rice. 2016: 9(1): 33. https://doi.org/10.1186/s12284-016-0107-4

Minh-Thu PT, Kim JS, Chae S, Jun KM, Lee GS, Kim DE, Cheong JJ, Song SI, Nahm BH, Kim YK. A WUSCHEL homeobox transcription factor, OsWOX13, enhances drought tolerance and triggers early flowering in rice. Mol. Cells. 2018: 41(8): 781–798. https://doi.org/10.14348/molcells.2018.0203

Muhammad TS, Pan ZE, He SP, Chen BJ, Km Y, Mahmood T, Sadau SB, Iqbal MS, Gereziher T, Abubakar US, et al. Characterization of *WOX* genes revealed drought tolerance, callus induction,

and tissue regeneration in *Gossypium hirsutum*. Front Genet. 2022: 13: 928055. https://doi.org/10.3389/fgene.2022.928055

Ryu CH, Lee S, Cho LH, Kim SL, Lee YS, Choi SC, Jeong HJ, Yi J, Park SJ, Han CD, et al. OsMADS50 and OsMADS56 function antagonistically in regulating long day (LD)-dependent flowering in rice. Plant Cell Environ. 2009: 32(10): 1412–1427. https://doi.org/10.1111/j.1365-3040.2009.02008.x

Sun CH, Fang J, Zhao TL, Xu B, Zhang FT, Liu LC, Tang JY, Zhang GF, Deng XJ, Chen F, et al. The histone methyltransferase SDG724 mediates H3K36me2/3 deposition at *MADS50* and *RFT1* and promotes flowering in rice. Plant Cell. 2012: 24(8): 3235–3247. https://doi.org/10.1105/tpc.112.101436

Sun KL, Zong WB, Xiao DD, Wu ZQ, Guo XT, Li FQ, Song YG, Li ST, Wei GL, Hao Y, et al. Effects of the core heading date genes *Hd1*, *Ghd7*, *DTH8*, and *PRR37* on yield-related traits in rice. Theor Appl Genet. 2023: 136(11): 227. https://doi.org/10.1007/s00122-023-04476-x

Tan JJ, Jin MN, Wang JC, Wu FQ, Sheng PK, Cheng ZJ, Wang JL, Zheng XM, Chen LP, Wang Min, et al. *OsCOL10*, a CONSTANS-Like gene, functions as a flowering time repressor downstream of *Ghd7* in Rice. Plant Cell Physiol. 2016: 57(4): 798–812. https://doi.org/10.1093/pcp/pcw025

Tsuji H, Taoka KI, Shimamoto K. Regulation of flowering in rice: two florigen genes, a complex gene network, and natural variation. Curr Opin Plant Biol. 2010: 14(1): 45–52. https://doi.org/10.1016/j.pbi.2010.08.016

Tao FL, Zhang Z, Shi WJ, Liu YJ, Xiao DP, Zhang S, Zhu Z, Wang M, Liu FS. Single rice growth period was prolonged by cultivars shifts, but yield was damaged by climate change during 1981-2009 in China, and late rice was just opposite. Glob Chang Biol. 2013: 19(10): 3200–3209. https://doi.org/10.1111/gcb.12250

Van der Graaff E, Laux T, Rensing SA. The WUS homeobox-containing (WOX) protein family. Genome Biol. 2009: 10(12): 248. https://doi.org/10.1186/gb-2009-10-12-248

Waadt R, Kudla J. In planta visualization of protein interactions using bimolecular fluorescence complementation (BiFC). CSH Protoc. 2008: pdb.prot4995. https://doi.org/10.1101/pdb.prot4995

Wang WS, Mauleon R, Hu ZQ, Chebotarov D, Tai SS, Wu ZC, Li M, Zheng TQ, Fuentes RR, Zhang F, et al. Genomic variation in 3,010 diverse accessions of Asian cultivated rice. Nature. 2018: 557(7703): 43–49. https://doi.org/10.1038/s41586-018-0063-9

Wei XJ, Xu JF, Guo HN, Jiang L, Chen SH, Yu CY, Zhou ZL, Hu PS, Zhai HQ, Wan JM. DTH8 suppresses flowering in rice, influencing plant height and yield potential simultaneously. Plant Physiol. 2010: 153(4): 1747–1758. https://doi.org/10.1104/pp.110.156943

Wu CY, You CJ, Li CS, Long T, Chen GX, Byrne ME, Zhang QF. RID1, encoding a Cys2/His2-type zinc finger transcription factor, acts as a master switch from vegetative to floral development in rice. Proc Natl Acad Sci U S A. 2008: 105(35): 12915–12920. https://doi.org/10.1073/pnas.0806019105

Xue WY, Xing YZ, Weng XY, Zhao Y, Tang WJ, Wang L, Zhou HJ, Yu SB, Xu CG, Li XH, et al. Natural variation in Ghd7 is an important regulator of heading date and yield potential in rice. Nat Genet. 2008: 40(6): 761–767. https://doi.org/10.1038/ng.143

Xu F, Tang JY, Wang SX, Cheng X, Wang HR, Ou SJ, Gao SP, Li BS, Qian YW, Gao CX, et al. Antagonistic control of seed dormancy in rice by two bHLH transcription factors. e. 2022: 54(12): 1972–1982. https://doi.org/10.1038/s41588-022-01240-7

Xu P, Zhang YX, Wen XX, Yang QQ, Liu L, Hao SL, Li JX, Wu ZZ, Shah L, Sohail A, et al. The clock component OsLUX regulates rice heading through recruiting OsELF3-1 and OsELF4s to repress *Hd1* and *Ghd7*. J Adv Res. 2023: 48: 17–31. https://doi.org/10.1016/j.jare.2022.08.001

Yokoo T, Saito H, Yoshitake Y, Xu Q, Asami T, Tsukiyama T, Teraishi M, Okumoto Y, Tanisaka T. Se14, encoding a JmjC domain-containing protein, plays key roles in long-day suppression of rice flowering through the demethylation of H3K4me3 of RFT1. PLoS One. 2014: 9(4): e96064. https://doi.org/10.1371/journal.pone.0096064

Zhang JH, Lin QB, Wang X, Shao JL, Ren YL, Liu X, Feng M, Li S, Sun Q, Luo S, et al. The DENSE AND ERECT PANICLE1-GRAIN NUMBER ASSOCIATED module enhances rice yield by repressing *CYTOKININ OXIDASE 2* expression. Plant Cell. 2025: 37(1): koae309. https://doi.org/10.1093/plcell/koae309

Zhang XN, Feng Q, Miao JS, Zhu JJ, Zhou CC, Fan DL, Lu YQ, Tian QL, Wang YC, Zhan QL, et al. The WD40 domain-containing protein Ehd5 positively regulates flowering in rice (*Oryza sativa*). Plant Cell. 2023: 35(11): 4002–4019. https://doi.org/10.1093/plcell/koad223

Zhang Y, Su JB, Duan S, Ao Y, Dai JR, Liu J, Wang P, Li YG, Liu B, Feng DR, et al. A highly efficient rice green tissue protoplast system for transient gene expression and studying light/chloroplast-related processes. Plant Methods. 2011: 7(1): 30. https://doi.org/10.1186/1746-4811-7-30

Zhao J, Chen HY, Ren D, Tang HW, Qiu R, Feng JL, Long YM, Niu BX, Chen DP, Zhong TY, et al. Genetic interactions between diverged alleles of *Early heading date 1* (*Ehd1*) and *Heading date 3a* (*Hd3a*)/ *RICE FLOWERING LOCUS T1* (*RFT1*) control differential heading and contribute to regional adaptation in rice (*Oryza sativa*). New phytol. 2015: 208(3): 936–948. https://doi.org/10.1111/nph.13503

Zheng XM, Feng L, Wang JR, Qiao WH, Zhang LF, Cheng YL, Yang QW. Nonfunctional alleles of long-day suppressor genes independently regulate flowering time. J Integr Plant Biol. 2016: 58(6): 540–548. https://doi.org/10.1111/jipb.12383

Zhou SR, Cai L, Wu HQ, Wang BX, Gu B, Cui S, Huang XL, Zhuang X, Hao BY, Hou HG, et al. Fine-tuning rice heading date through multiplex editing of the regulatory regions of key genes by CRISPR-Cas9. Plant Biotechnol J. 2024: 22(3): 751–758. https://doi.org/10.1111/pbi.14221

Zhu SS, Wang JC, Cai MH, Zhang H, Wu FQ, Yang X, Li CN, Cheng ZJ, Zhang X, Guo XP, et al. The OsHAPL1-DTH8-Hd1 complex functions as the transcription regulator to repress heading date in rice. J Exp Bot. 2017: 68(3): 553–568. https://doi.org/10.1093/jxb/erw468

Figure 1. Ehd1 binds to *OsWOX13* promoter and activates its expression. **A)** Schematic of the *OsWOX13* gene structure. Black squares, blue thick lines, and thin lines represent exons, introns, and promoters, respectively. P1, named *OsWOX13-P1*, includes a 2000 bp upstream sequence of the ATG start codon, the ATG itself, and a 69 bp downstream fragment identified by ChIP-Seq. P2, named *OsWOX13-P2*, was a fragment identified by ChIP-Seq and contains a 105 bp upstream sequence of the ATG start codon, the ATG itself, and a 69 bp downstream fragment. The red-labeled region in P2-2 corresponds to the overlapping segments of P2-2-2 with P2-2-1 and P2-2-3, respectively. The sequences of these two regions were mutated to generate P2-2

Mut-T and P2-2 Mut-G, which were used in the LUC and EMSA assays. **B)** ChIP-qPCR assays showed that Ehd1 was enriched in the *OsWOX13* promoter. The ChIP assays using *ProEhd1:Ehd1-GFP ehd1-2* line were conducted on leaves, according to the ChIP-Seq results. Nuclear proteins were immunoprecipitated with GFP antibody, and the enriched DNA was used for qPCR assays. *Actin* served as a negative control locus. Statistical analysis was performed using ANOVA followed by Tukey's test (P<0.05). Data are means ± SD (n = three independent experiments). **C)** Motif analysis of Ehd1-enriched *OsWOX13-P2* peak region. Known motif: the known binding motif of Ehd1. De novo motif: the predicted binding motif of Ehd1 identified by de novo motif analysis. **D)** EMSA assays analyzed that Ehd1 interacts with the *OsWOX13* promoter. The 10 bp overlap between O*sWOX13-P2-2-1* and *OsWOX13-P2-2-2* was mutated to 10 bp thymine (T) stretch, resulting in P2-2 mut probe-T, while the 10 bp overlap between *OsWOX13-P2-2-2* and *OsWOX13-P2-2-3* was mutated to 10 bp guanine (G) stretch, resulting in P2-2 mut probe-G. Both mut probe-T and mut probe-G were biotin-labeled. The arrow indicates the binding shift (n = three independent experiments). **E)** The transcription activities of the reporters were significantly activated by Ehd1. The 10 bp overlapping region between *OsWOX13-P2-2-1* and *OsWOX13-P2-2-2* was mutated to 10 bp T stretch to generate *OsWOX13-P2-2-Mut-T*, whereas the 10 bp overlap between *OsWOX13-P2-2-2* and *OsWOX13-P2-2-3* was mutated to a 10 bp G stretch to produce *OsWOX13-P2-2-Mut-G*. FLAG+*OsWOX13-P1/-P2/-P2-1/-P2-2/-P2-2-Mut-G/-P2-2-Mut-T/-P2-3/-P2-4* served as the control groups, while Ehd1-FLAG+*OsWOX13-P1/-P2/-P2-1/-P2-2/-P2-2-Mut-G/-P2-2-Mut-T/-P2-3/-P2-4* served as the experimental groups. Statistical analysis was performed using ANOVA followed by Tukey's test (P<0.05). Data are means ± SD (n = three independent experiments). **F** and **G)** The diurnal expression patterns of *OsWOX13* in leaves were analyzed in NIP, *Ehd1-OE* and *ehd1* within 48 hours under natural long-day (NLD) and short-day conditions (CSD) by qRT-PCR. The rice *ubiquitin* (*UBQ*) gene was used as the internal control. The black squares represent the dark period, while the black squares with white interiors represent the light period. Statistical analyses were performed separately on the measured data at each sampling time point using ANOVA followed by Tukey test (P<0.05). Data are means ± SD (n = three biological replicates).

Figure 2. Characterization of heading date in *Oswox13* mutants and *Oswox13 ehd1*. **A)** CRISPR/Cas9-mediated target mutagenesis of *OsWOX13*. Exons are indicated by black boxes, and introns by blue lines. The Sanger sequencing chromatograms show the mutation sites and types of the *OsWOX13* gene. **B** and **C)** Phenotypes of NIP, *OsWOX13-OE* lines and *Oswox13* mutants at heading date under NLD. At the developmental stage when the main panicles of NIP (**B**) or the *Oswox13* (**C**) had just emerged. Scale bar corresponds to 10 cm. **D** and **E)** Heading dates were calculated for NIP, *OsWOX13-OE* lines, and *Oswox13* under NLD (**D**) and NSD (**E**). Data are means ± SD (n = 30 plants). Statistical analysis was performed using ANOVA followed by Tukey's test (P<0.05). **F)** Phenotypic comparison between *Oswox13 ehd1* and *ehd1* at heading date under NLD. At the developmental stage when the main panicles of *Oswox13 ehd1*

and the *ehd1* had just emerged. Scale bar corresponds to 10 cm. **G** and **H)** Phenotypic analysis of heading date in *Oswox13 ehd1* under NLD (**G**) and NSD (**H**). Statistical analysis was performed using ANOVA followed by Tukey's test (P<0.05). Data are means ± SD (n = 30 plants).

Figure 3. OsWOX13 can bind to the promoter of *Hd3a,* and regulate its expression. **A)** The diagram shows the gene structure of *Hd3a*: black squares, blue thick lines, and thin lines represent exons, introns, and promoters, respectively. The construct designated as P1, named *Hd3a-P1*, includes a 2500 bp upstream sequence relative to the ATG start codon. The fragment designated as P2, named *Hd3a-P2*, consist of a 100 bp sequence that includes the motif CAATCAAT. P2 was further truncated into a 30-bp fragment (designated P3) containing the motif, which was then used for EMSA. **B)** A structure diagram of the recombinant vector was presented. The *Pro35S:*REN-*Hd3a-P1*-LUC, *Pro35S:*REN-*Hd3a-P2*-LUC construct function as a reporter, whereas the *Pro35S:FLAG* and *Pro35S:OsWOX13-FLAG* constructs serve as effectors, respectively. **C)** The transcription activities of the reporters were significantly activated by OsWOX13. The combination of FLAG and *Hd3a-P1/-P2* were designated as the control groups, while the pairing of OsWOX13-FLAG and *Hd3a-P1/-P2* were set as the experimental groups. Statistical analysis was performed using ANOVA followed by Tukey's test (P<0.05). Data are means ± SD (n = three independent experiments). **D)** ChIP assays showed that OsWOX13 was enriched in the *Hd3a* promoter. The ChIP assays were carried out on leaves using the *ProOsWOX13:OsWOX13-FLAG Oswox13-2* line. Nuclear proteins were immunoprecipitated with a FLAG antibody, and the enriched DNA was utilized for qPCR assays. *Actin* was employed as a negative control locus. The data were presented as means ± SD (n = three independent experiments). Statistical analysis was performed using ANOVA followed by Tukey's test (P<0.05). **E)** EMSA showed OsWOX13 directly bind to the *Hd3a* promoter. The labeled probe was equipped with a biotin tag, while the competitor lacked such a tag. CAATCAAT in the labeled probe sequence was mutated into GGGGGGGG, thus generating a mutant probe. The arrow indicates the binding shift (n = three independent experiments). **F** and **G)** The expression patterns of *Hd3a* in leaves were examined in NIP, *OsWOX13-OE* and *Oswox13* over a 48 h period under natural long-day (NLD) and short-day conditions (CSD) by qRT-PCR. The black squares represent the dark period, while the black squares with white interiors represent the light period. Data are means ± SD (n = three biological replicates).

Figure 4. The OsWOX13-Hd3a interaction inhibited OsWOX13 mediated activation of *Hd3a*. **A)** The BiFC experiment elucidated the interaction between OsWOX13 and Hd3a in *N. benthamiana* leaves (n = three independent experiments). OsWOX13-nYFP+cYFP-OsICE2, OsICE2-nYFP+cYFP-Hd3a were used as negative controls. D53-mCherry was used as a nuclear marker. **B)** The pulldown assays confirmed the interaction between OsWOX13 and Hd3a (n = three independent experiments). His-OsWOX13 and GST, His and GST-Hd3a or His-OsWOX13

and GST-Hd3a were co-incubated with His-tagged beads. The His-OsWOX13 and GST combination, as well as His and GST-Hd3a combination were served as negative controls. The symbols "+" and "-" represent the presence and absence of the corresponding proteins. **C)** An in vivo Co-IP assay validated the interaction between OsWOX13 and Hd3a (n = three independent experiments). Total protein extracts were incubated with anti-FLAG beads. OsWOX13-FLAG+GFP and Hd3a-GFP were used as negative controls. The symbols "+" and "-" represent the presence and absence of the corresponding proteins. **D)** The structure of the recombinant vector was illustrated. The *Pro35S:*REN-*Hd3a-P1*-LUC construct functions as a reporter, whereas the *Pro35S:FLAG*, *Pro35S:OsWOX13-FLAG*, *Pro35S:GFP* and *Pro35S:Hd3a-GFP* constructs serve as effectors, respectively. **E)** The transcription activities of the reporters were significantly repressed by Hd3a in protoplasts of the *hd3a*. The combination of FLAG, GFP, and *Hd3a-P1* was used as the control group, whereas OsWOX13-FLAG with *Hd3a-P1* in conjunction with either GFP or Hd3a-GFP served as the experimental groups. Statistical analysis was performed using ANOVA followed by Tukey's test ($P<0.05$). Data are means ± SD (n = three independent experiments). **F)** ChIP assays revealed that Hd3a represses the enrichment of OsWOX13 on its own promoter. *ProOsWOX13:OsWOX13-FLAG* was transformed into protoplasts of NIP and the *hd3a* mutant for ChIP assays. Nuclear proteins were immunoprecipitated with a FLAG antibody, and the enriched DNA was utilized for qPCR assays. *Actin* was employed as a negative control locus. Statistical analysis was performed using ANOVA followed by Tukey's test ($P<0.05$). The data were presented as means ± SD (n = three independent experiments). **G)** EMSA results showed that Hd3a inhibits the binding of OsWOX13 to *Hd3a-P3* (n = three independent experiments). The labeled probe was equipped with a biotin tag. His+labeled probe and His-Hd3a+labeled probe were used as the control groups. **H**) The endogenous *Hd3a* expression level in protoplasts was identified. OsWOX13-FLAG+GFP and OsWOX13-FLAG+Hd3a-GFP were separately transformed into protoplasts for expression, with OsWOX13+GFP serving as the control group and HSP82 as the internal reference protein; qRT-PCR primers were designed in the 3' UTR region of *Hd3a* to identify the relative expression levels of endogenous *Hd3a*. The relative expression level of *Hd3a* was assessed using $2^{-\Delta\Delta CT}$ method. Significance was assessed using a two-tailed Student's *t*-test. Data are means ± SD (n = three biological replicates). **I)** The expression patterns of *Hd3a* in leaves were examined in NIP and *hd3a* over a 48 h period under short-day conditions by qRT-PCR. The black squares represent the dark period, while the black squares with white interiors represent the light period. Data are means ± SD (n = three biological replicates).

Figure 5. *OsWOX13* genetically interacts with *Hd3a* to regulate heading date. **A)** CRISPR/Cas9-mediated target mutagenesis of *Hd3a*. Exons are indicated by black boxes, and introns by blue lines. The Sanger sequencing chromatograms show the mutation sites and types of the *Hd3a*. **B)** Phenotypic characteristics of NIP, *Oswox13-2*, *hd3a-1*, *Oswox13-2 hd3a-1* and *Oswox13-2 hd3a-2* at heading date under NLD conditions. At the developmental stage when the main panicles of

hd3a had just emerged. Scale bar corresponds to 10 cm. **C** and **D)** Heading dates were calculated for NIP, *Oswox13-2*, *hd3a-1*, *Oswox13-2 hd3a-1* and *Oswox13-2 hd3a-2* under NLD (**C**) and NSD (**D**). **E)** Phenotypic characteristics of NIP, *OsWOX13-OE-3*, *hd3a-1*, *OsWOX13-OE-3 hd3a-1* and *OsWOX13-OE-3 hd3a-2* at heading date under NLD conditions. At the developmental stage when the main panicles of *hd3a* had just emerged. Scale bar corresponds to 10 cm. **F** and **G)** Heading dates were calculated for NIP, *OsWOX13-OE-3*, *hd3a-1*, *OsWOX13-OE-3 hd3a-1* and *OsWOX13-OE-3 hd3a-2* under NLD (**F**) and NSD (**G**). Data are means ± SD (n = 30 plants). Statistical analysis was performed using ANOVA followed by Tukey's test (P<0.05) (**C** to **G**).

Figure 6. The *Hap-T* haplotype promoted rice heading by increasing the expression levels of *OsWOX13* and *Hd3a*. **A)** Linkage analysis was performed between the haplotype at the -54 bp position of the *OsWOX13* gene promoter (Chr 1: 34863184) and heading date in natural populations. The total number of varieties was 2792. The frequencies of the *Hap-T* and *Hap-C* were 33.7% and 64.4%, respectively, whereas *Hap-Y*, corresponding to the heterozygous genotype, exhibited a frequency of 1.9%. Statistical significance of heading date between rice varieties carrying *Hap-T* and those carrying *Hap-C* was analyzed using a two-tailed Student's *t* test. (P = 4.64E-05). **B** and **C)** Heading dates were calculated for Longjing 31, Longjing $31^{T\text{-}C}$-1 and Longjing $31^{T\text{-}C}$-2 under CLD (**B**) and CSD (**C**). Longjing $31^{T\text{-}C}$ represents the genotype where the thymine (T) residues at positions 34863184 and 34863187 on chromosome 1 are both mutated to cytosine (C). Data are means ± SD (n = 30 plants). Statistical analysis was performed using ANOVA followed by Tukey's test (P<0.05). **D)** Structure diagram of recombinant vector. The *Pro35S:*REN-*OsWOX13-P1T*-LUC and *Pro35S:*REN-*OsWOX13-P1C*-LUC constructs serve as reporters, while the *Pro35S:Ehd1-FLAG* and *Pro35S:FLAG* construct serves as effectors, respectively. **E)** The LUC assay analyzed the activation ability of Ehd1 on *OsWOX13* promoters with different haplotypes. Both *OsWOX13-P1T* and *OsWOX13-P1C* encompass the 2000 bp upstream sequence of the *OsWOX13* promoter, with *OsWOX13-P1T* harboring a T and *OsWOX13-P1C* a C at the -54 bp position (Chr 1: 34863184). HSP82 as the internal reference protein. Statistical analysis was performed using ANOVA followed by Tukey's test (P<0.05). Data are means ± SD (n = three independent experiments). **F)** The EMSA assay analyzed the binding ability of Ehd1 on *OsWOX13* promoters with different haplotypes (n = three independent experiments). The sequences of labeled probes *P2-2* and *P2-2-T* were identical, with a T at the -54 bp position, whereas labeled probes *P2-2-C* differed only at the -54 bp position, where it had a C. **G** to **N)** The expression levels of *OsWOX13* and *Hd3a* in different haplotypes were analyzed (n = three biological replicates). Forty rice varieties each of *Hap-T* and *Hap-C* were randomly selected. After being grow for 25 days under CSD conditions and 50 days under CLD conditions, the expression levels of *OsWOX13* (**G** and **H**) and *Hd3a* (**I** and **J**) in leaves were determined by qRT-PCR. Data are means ± SD (n = 40 plants). Longjing 31, Longjing $31^{T\text{-}C}$-1 and Longjing $31^{T\text{-}C}$-2 were grown under CSD and CLD for 35 and 45 days, respectively, followed by the

determination of the expression levels of *OsWOX13* (**K** and **L**) and *Hd3a* (**M** and **N**) in leaves. The relative expression levels of *OsWOX13* and *Hd3a* were assessed using $2^{-\Delta\Delta CT}$ method. Data are presented as mean ± SD (n = three biological replicates). Statistical analysis was performed using two-tailed Student's *t* test (**G** to **J**) and ANOVA followed by Tukey's test ($P<0.05$) (**K** to **N**).

Figure 7. The geographical distribution of *Hap-T* and *Hap-C*. **A** and **B)** The geographical distribution of the two haplotypes, *Hap-T* and *Hap-C*, was investigated worldwide and across Asia. The sample sizes for the *Hap-T* and *Hap-C* were 942 and 1797 rice accessions, respectively. Green indicates the presence of the *Hap-C* haplotype, while red represents the *Hap-T* haplotype. Pie charts were used to illustrate the proportions of *Hap-T* and *Hap-C* haplotypes. The dotted lines represent longitude and latitude.

Figure 8. Model of *Ehd1-OsWOX13-Hd3a* pathway regulation of heading date in rice. Ehd1 exhibits a stronger activation effect on *OsWOX13* expression in the *Hap-T*. OsWOX13 binds to the *Hd3a* promoter and activates its expression; moreover, the interaction between OsWOX13 and Hd3a weakens the activation of *Hd3a* expression, that precisely modulates *Hd3a* transcription and indirectly regulates the level of *RFT1*. Ultimately, *OsWOX13* in the *Hap-T* shows higher expression, leading to elevated florigen levels and thus promoting heading in rice.

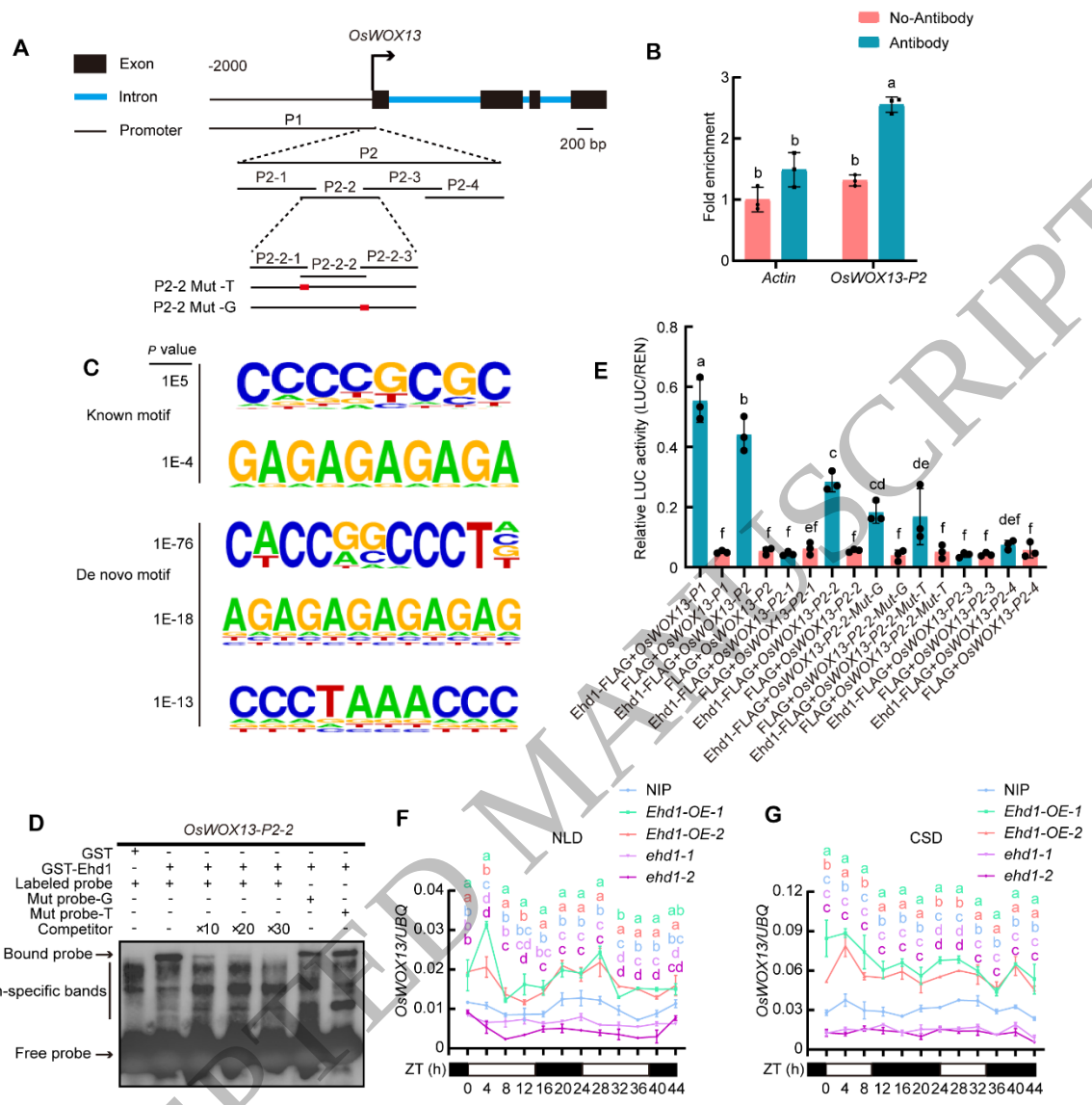

Figure 1. Ehd1 binds to *OsWOX13* promoter and activates its expression. **A)** Schematic of the *OsWOX13* gene structure. Black squares, blue thick lines, and thin lines represent exons, introns, and promoters, respectively. P1, named *OsWOX13-P1*, includes a 2000 bp upstream sequence of the ATG start codon, the ATG itself, and a 69 bp downstream fragment identified by ChIP-Seq. P2, named *OsWOX13-P2*, was a fragment identified by ChIP-Seq and contains a 105 bp upstream sequence of the ATG start codon, the ATG itself, and a 69 bp downstream fragment. The red-labeled region in P2-2 corresponds to the overlapping segments of P2-2-2 with P2-2-1 and P2-2-3, respectively. The sequences of these two regions were mutated to generate P2-2 Mut-T and P2-2 Mut-G, which were used in the LUC and EMSA assays. **B)** ChIP-qPCR assays showed that Ehd1 was enriched in the *OsWOX13* promoter. The ChIP assays using *ProEhd1:Ehd1-GFP ehd1-2* line were conducted on leaves, according to the ChIP-Seq results. Nuclear proteins were immunoprecipitated with GFP antibody, and the enriched DNA was used for qPCR assays. *Actin* served as a negative control locus. Statistical analysis was performed using ANOVA followed by Tukey's test (P<0.05). Data are means ± SD (n = three independent experiments). **C)** Motif analysis of Ehd1-enriched *OsWOX13-P2* peak region. Known motif: the known binding motif of Ehd1. De novo motif: the predicted binding motif of Ehd1 identified by de novo motif analysis. **D)** EMSA assays analyzed that Ehd1 interacts with the *OsWOX13* promoter. The 10 bp overlap between O*sWOX13-P2-2-1* and *OsWOX13-P2-2-2* was mutated to 10 bp thymine (T) stretch, resulting in P2-2 mut probe-T, while the 10 bp overlap between *OsWOX13-P2-2-2* and *OsWOX13-P2-2-3* was mutated to 10 bp guanine (G) stretch, resulting in P2-2 mut probe-G. Both mut probe-T and mut probe-G were biotin-labeled. The arrow indicates the binding shift (n = three independent experiments). **E)** The transcription activities of the reporters were significantly activated by Ehd1. The 10 bp overlapping region between *OsWOX13-P2-2-1* and *OsWOX13-P2-2-2* was mutated to 10 bp T stretch to generate *OsWOX13-P2-2-Mut-T*, whereas the 10 bp overlap between *OsWOX13-P2-2-2* and *OsWOX13-P2-2-3* was mutated to a 10 bp G stretch to produce *OsWOX13-P2-2-Mut-G*. FLAG+*OsWOX13-P1/-P2/-P2-1/-P2-2/-P2-2-Mut-G/-P2-2-Mut-T/-P2-3/-P2-4* served as the control groups, while Ehd1-FLAG+*OsWOX13-P1/-P2/-P2-1/-P2-2/-P2-2-Mut-G/-P2-2-Mut-T/-P2-3/-P2-4* served as the experimental groups. Statistical analysis was performed using ANOVA followed by Tukey's test (P<0.05). Data are means ± SD (n = three independent experiments). **F** and **G)** The diurnal expression patterns of *OsWOX13* in leaves were analyzed in NIP, *Ehd1-OE* and *ehd1* within 48 hours under natural long-day (NLD) and short-day conditions (CSD) by qRT-PCR. The rice *ubiquitin* (*UBQ*) gene was used as the internal control. The black squares represent the dark period, while the black squares with white interiors represent the light period. Statistical analyses were performed separately on the measured data at each sampling time point using ANOVA followed by Tukey test (P<0.05). Data are means ± SD (n = three biological replicates).

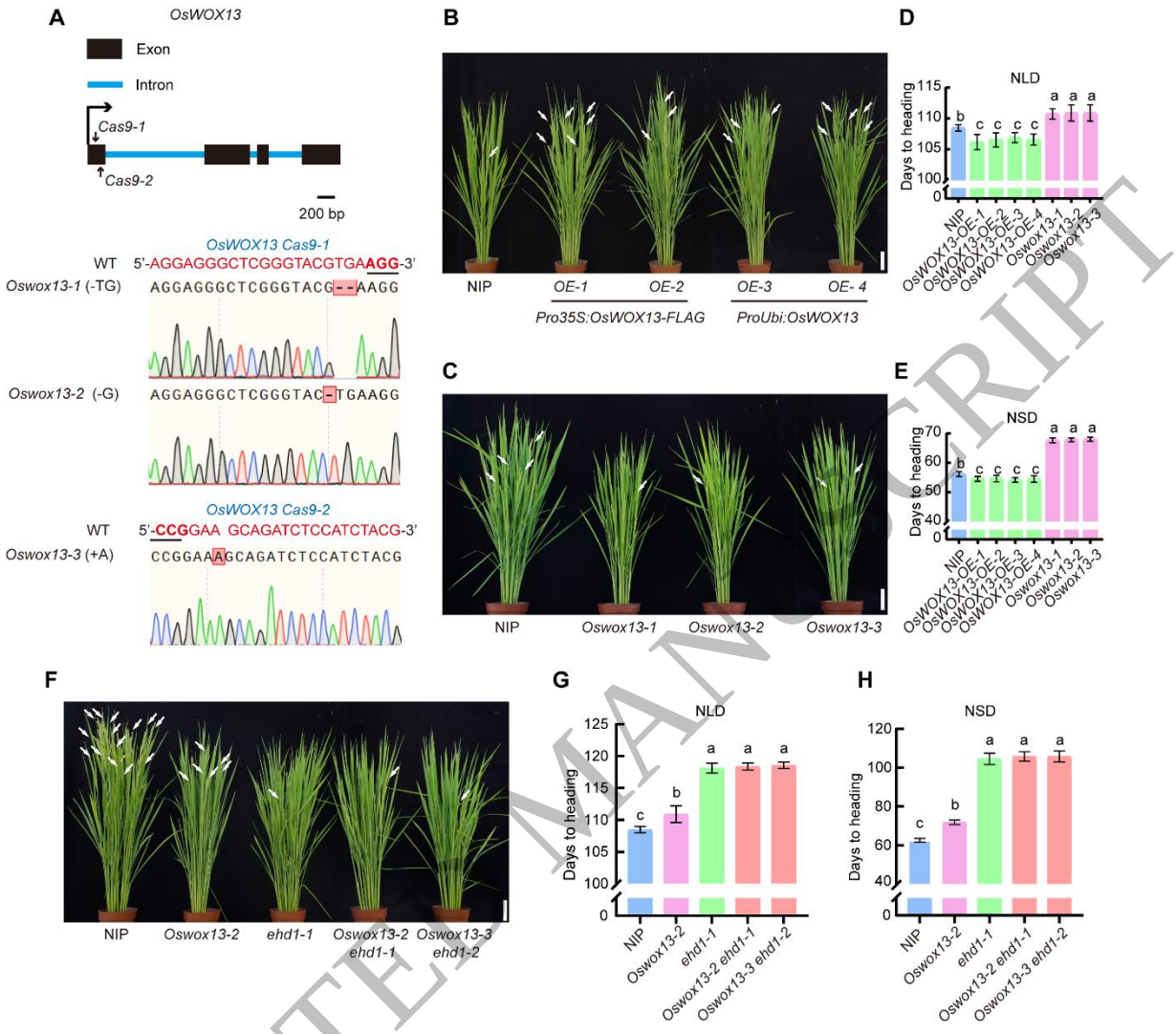

Figure 2. Characterization of heading date in *Oswox13* mutants and *Oswox13 ehd1*. **A)** CRISPR/Cas9-mediated target mutagenesis of *OsWOX13*. Exons are indicated by black boxes, and introns by blue lines. The Sanger sequencing chromatograms show the mutation sites and types of the *OsWOX13* gene. **B** and **C)** Phenotypes of NIP, *OsWOX13-OE* lines and *Oswox13* mutants at heading date under NLD. At the developmental stage when the main panicles of NIP (**B**) or the *Oswox13* (**C**) had just emerged. Scale bar corresponds to 10 cm. **D** and **E)** Heading dates were calculated for NIP, *OsWOX13-OE* lines, and *Oswox13* under NLD (**D**) and NSD (**E**). Data are means ± SD (n = 30 plants). Statistical analysis was performed using ANOVA followed by Tukey's test (P<0.05). **F)** Phenotypic comparison between *Oswox13 ehd1* and *ehd1* at heading date under NLD. At the developmental stage when the main panicles of *Oswox13 ehd1* and the *ehd1* had just emerged. Scale bar corresponds to 10 cm. **G** and **H)** Phenotypic analysis of heading date in *Oswox13 ehd1* under NLD (**G**) and NSD (**H**). Statistical analysis was performed using ANOVA followed by Tukey's test (P<0.05). Data are means ± SD (n = 30 plants).

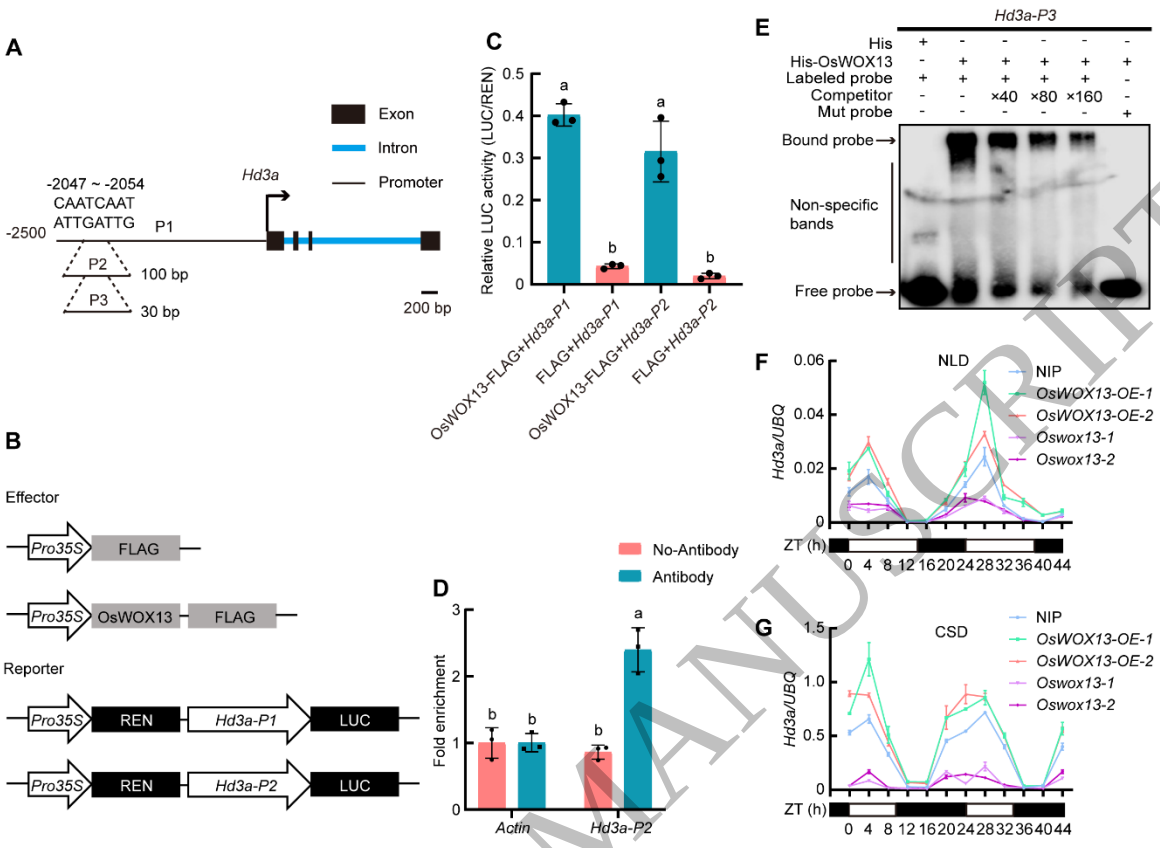

Figure 3. OsWOX13 can bind to the promoter of *Hd3a,* and regulate its expression. **A)** The diagram shows the gene structure of *Hd3a*: black squares, blue thick lines, and thin lines represent exons, introns, and promoters, respectively. The construct designated as P1, named *Hd3a-P1*, includes a 2500 bp upstream sequence relative to the ATG start codon. The fragment designated as P2, named *Hd3a-P2*, consist of a 100 bp sequence that includes the motif CAATCAAT. P2 was further truncated into a 30-bp fragment (designated P3) containing the motif, which was then used for EMSA. **B)** A structure diagram of the recombinant vector was presented. The *Pro35S:*REN-*Hd3a-P1*-LUC, *Pro35S:*REN-*Hd3a-P2*-LUC construct function as a reporter, whereas the *Pro35S:FLAG* and *Pro35S:OsWOX13-FLAG* constructs serve as effectors, respectively. **C)** The transcription activities of the reporters were significantly activated by OsWOX13. The combination of FLAG and *Hd3a-P1/-P2* were designated as the control groups, while the pairing of OsWOX13-FLAG and *Hd3a-P1/-P2* were set as the experimental groups. Statistical analysis was performed using ANOVA followed by Tukey's test ($P<0.05$). Data are means ± SD (n = three independent experiments). **D)** ChIP assays showed that OsWOX13 was enriched in the *Hd3a* promoter. The ChIP assays were carried out on leaves using the *ProOsWOX13:OsWOX13-FLAG Oswox13-2* line. Nuclear proteins were immunoprecipitated with a FLAG antibody, and the enriched DNA was utilized for qPCR assays. *Actin* was employed as a negative control locus. The data were presented as means ± SD (n = three independent experiments). Statistical analysis was performed using ANOVA followed by

Tukey's test (P<0.05). **E)** EMSA showed OsWOX13 directly bind to the *Hd3a* promoter. The labeled probe was equipped with a biotin tag, while the competitor lacked such a tag. CAATCAAT in the labeled probe sequence was mutated into GGGGGGGG, thus generating a mutant probe. The arrow indicates the binding shift (n = three independent experiments). **F** and **G)** The expression patterns of *Hd3a* in leaves were examined in NIP, *OsWOX13-OE* and *Oswox13* over a 48 h period under natural long-day (NLD) and short-day conditions (CSD) by qRT-PCR. The black squares represent the dark period, while the black squares with white interiors represent the light period. Data are means ± SD (n = three biological replicates).

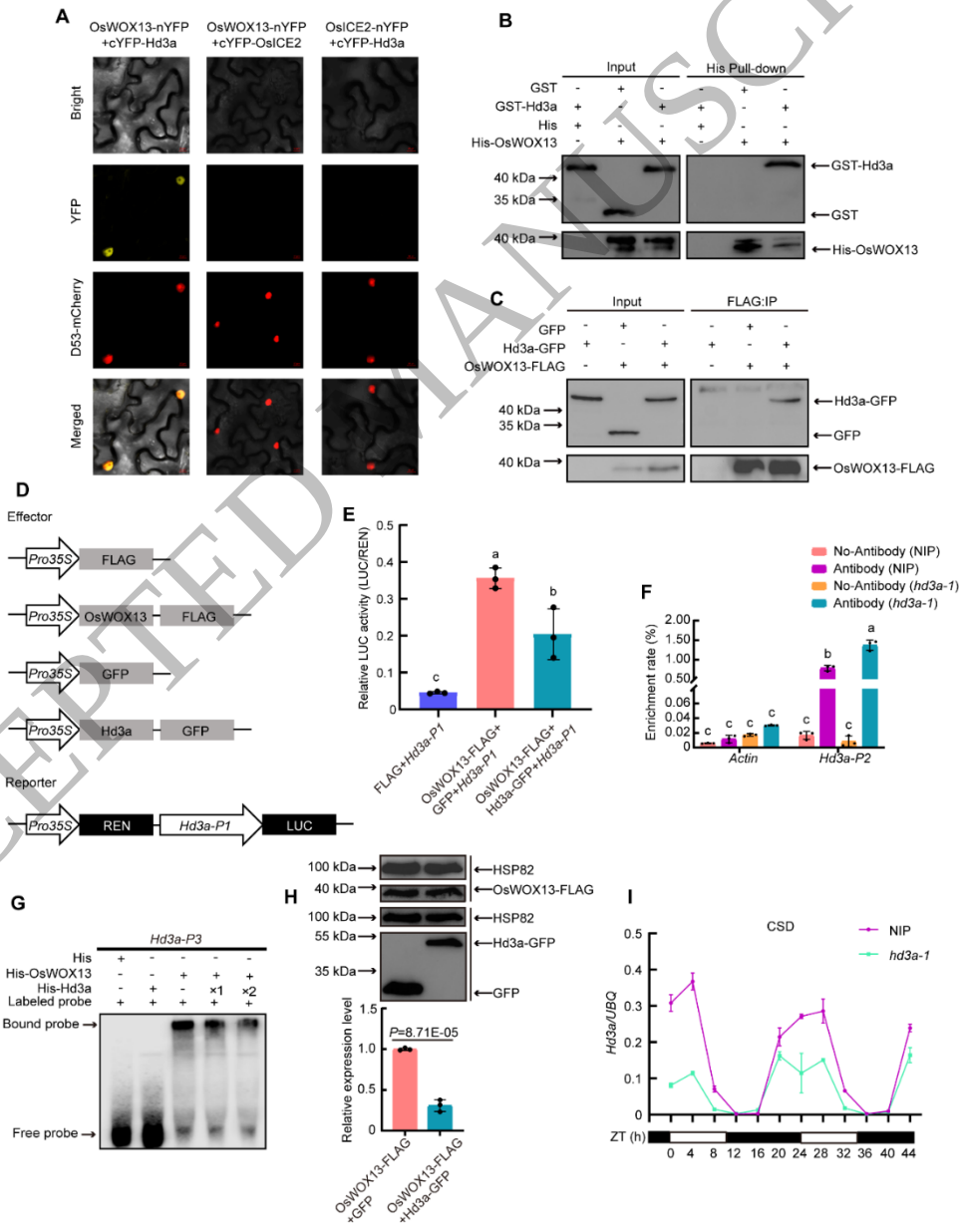

Figure 4. The OsWOX13-Hd3a interaction inhibited OsWOX13 mediated activation of *Hd3a*. **A)** The BiFC experiment elucidated the interaction between OsWOX13 and Hd3a in *N. benthamiana* leaves (n = three independent experiments). OsWOX13-nYFP+cYFP-OsICE2, OsICE2-nYFP+cYFP-Hd3a were used as negative controls. D53-mCherry was used as a nuclear marker. **B)** The pulldown assays confirmed the interaction between OsWOX13 and Hd3a (n = three independent experiments). His-OsWOX13 and GST, His and GST-Hd3a or His-OsWOX13 and GST-Hd3a were co-incubated with His-tagged beads. The His-OsWOX13 and GST combination, as well as His and GST-Hd3a combination were served as negative controls. The symbols "+" and "-" represent the presence and absence of the corresponding proteins. **C)** An in vivo Co-IP assay validated the interaction between OsWOX13 and Hd3a (n = three independent experiments). Total protein extracts were incubated with anti-FLAG beads. OsWOX13-FLAG+GFP and Hd3a-GFP were used as negative controls. The symbols "+" and "-" represent the presence and absence of the corresponding proteins. **D)** The structure of the recombinant vector was illustrated. The *Pro35S:*REN-*Hd3a-P1*-LUC construct functions as a reporter, whereas the *Pro35S:FLAG*, *Pro35S:OsWOX13-FLAG*, *Pro35S:GFP* and *Pro35S:Hd3a-GFP* constructs serve as effectors, respectively. **E)** The transcription activities of the reporters were significantly repressed by Hd3a in protoplasts of the *hd3a*. The combination of FLAG, GFP, and *Hd3a-P1* was used as the control group, whereas OsWOX13-FLAG with *Hd3a-P1* in conjunction with either GFP or Hd3a-GFP served as the experimental groups. Statistical analysis was performed using ANOVA followed by Tukey's test ($P<0.05$). Data are means ± SD (n = three independent experiments). **F)** ChIP assays revealed that Hd3a represses the enrichment of OsWOX13 on its own promoter. *ProOsWOX13:OsWOX13-FLAG* was transformed into protoplasts of NIP and the *hd3a* mutant for ChIP assays. Nuclear proteins were immunoprecipitated with a FLAG antibody, and the enriched DNA was utilized for qPCR assays. *Actin* was employed as a negative control locus. Statistical analysis was performed using ANOVA followed by Tukey's test ($P<0.05$). The data were presented as means ± SD (n = three independent experiments). **G)** EMSA results showed that Hd3a inhibits the binding of OsWOX13 to *Hd3a-P3* (n = three independent experiments). The labeled probe was equipped with a biotin tag. His+labeled probe and His-Hd3a+labeled probe were used as the control groups. **H**) The endogenous *Hd3a* expression level in protoplasts was identified. OsWOX13-FLAG+GFP and OsWOX13-FLAG+Hd3a-GFP were separately transformed into protoplasts for expression, with OsWOX13+GFP serving as the control group and HSP82 as the internal reference protein; qRT-PCR primers were designed in the 3' UTR region of *Hd3a* to identify the relative expression levels of endogenous *Hd3a*. The relative expression level of *Hd3a* was assessed using $2^{-\Delta\Delta CT}$ method. Significance was assessed using a two-tailed Student's *t*-test. Data are means ± SD (n = three biological replicates). **I)** The expression patterns of *Hd3a* in leaves were examined in NIP and *hd3a* over a 48 h period under short-day conditions by qRT-PCR. The black squares represent the dark period, while the black squares with white interiors represent the light period. Data are means ± SD (n = three biological replicates).

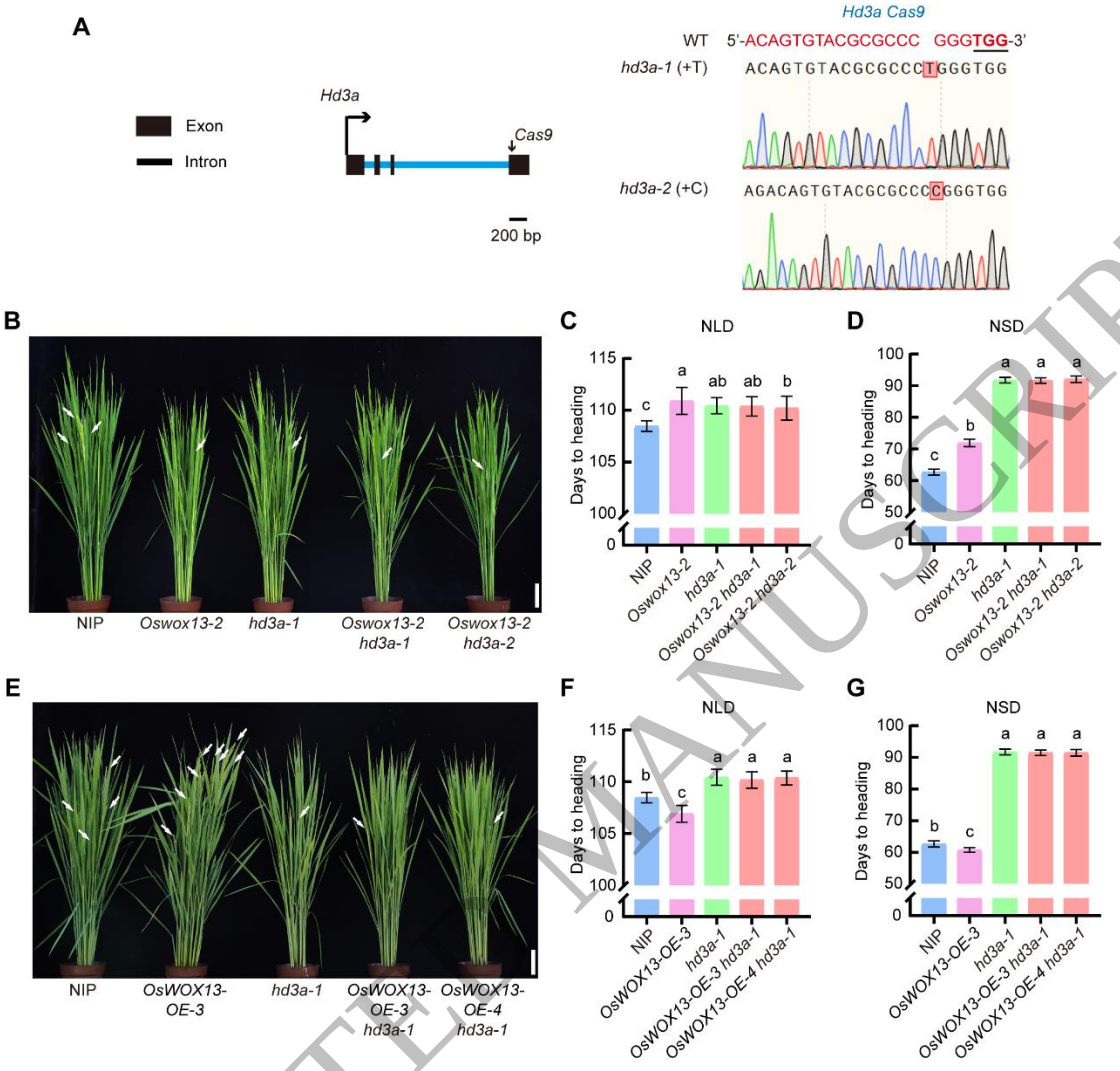

Figure 5. *OsWOX13* genetically interacts with *Hd3a* to regulate heading date. **A)** CRISPR/Cas9-mediated target mutagenesis of *Hd3a*. Exons are indicated by black boxes, and introns by blue lines. The Sanger sequencing chromatograms show the mutation sites and types of the *Hd3a*. **B)** Phenotypic characteristics of NIP, *Oswox13-2*, *hd3a-1*, *Oswox13-2 hd3a-1* and *Oswox13-2 hd3a-2* at heading date under NLD conditions. At the developmental stage when the main panicles of *hd3a* had just emerged. Scale bar corresponds to 10 cm. **C** and **D)** Heading dates were calculated for NIP, *Oswox13-2*, *hd3a-1*, *Oswox13-2 hd3a-1* and *Oswox13-2 hd3a-2* under NLD (**C**) and NSD (**D**). **E)** Phenotypic characteristics of NIP, *OsWOX13-OE-3*, *hd3a-1*, *OsWOX13-OE-3 hd3a-1* and *OsWOX13-OE-3 hd3a-2* at heading date under NLD conditions. At the developmental stage when the main panicles of *hd3a* had just emerged. Scale bar corresponds to 10 cm. **F** and **G)** Heading dates were calculated for NIP, *OsWOX13-OE-3*, *hd3a-1*, *OsWOX13-OE-3 hd3a-1* and *OsWOX13-OE-3 hd3a-2* under NLD (**F**) and NSD (**G**). Data are means ± SD (n = 30 plants). Statistical analysis was performed using ANOVA followed by Tukey's test (P<0.05) (**C** to **G**).

A

Haplotypes	Variety number	Days to heading
Hap-C	1797	mean: 95.974
Hap-T	942	mean: 93.733
Hap-Y	53	mean: 94.066

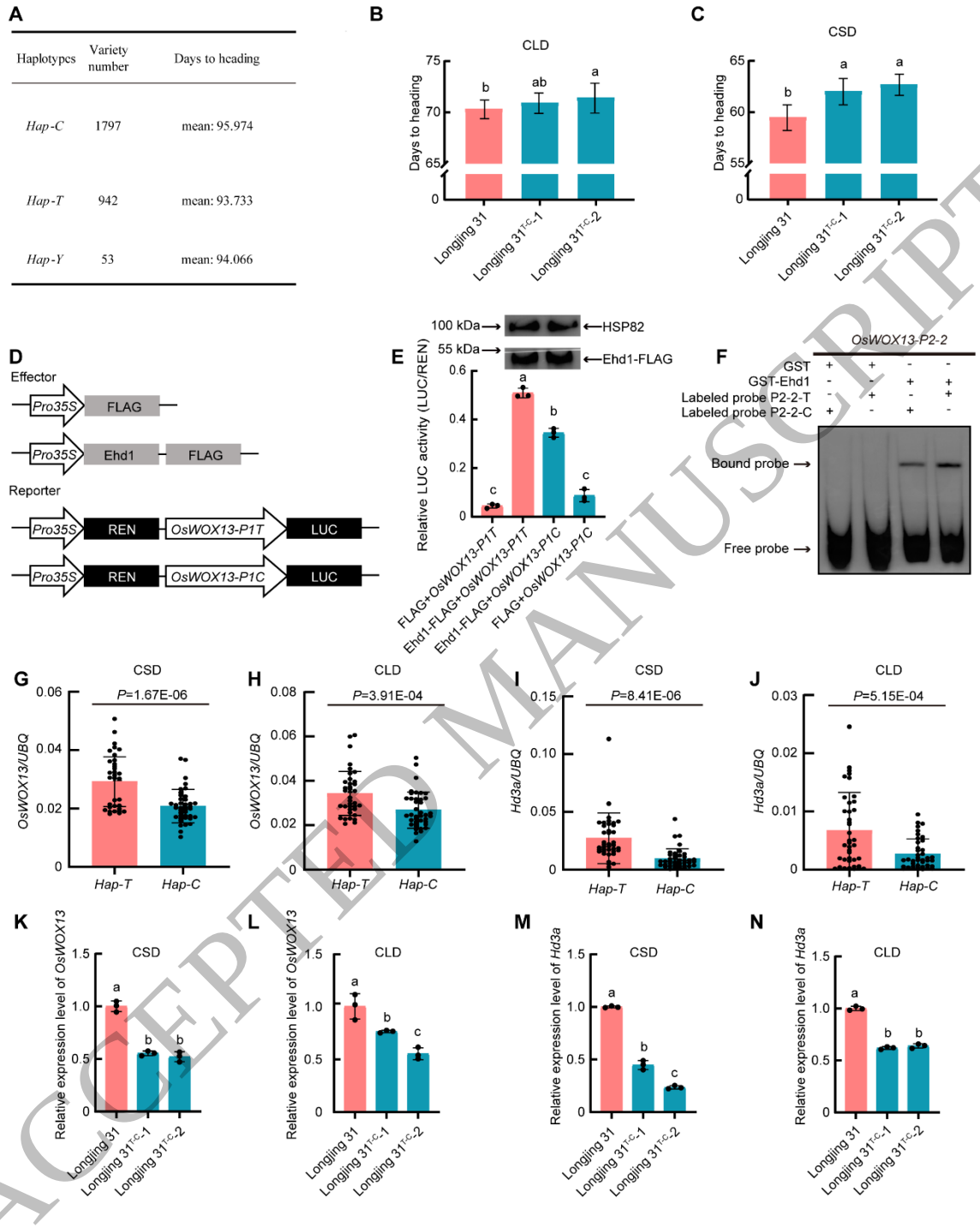

Figure 6. The *Hap-T* haplotype promoted rice heading by increasing the expression levels of *OsWOX13* and *Hd3a*. **A)** Linkage analysis was performed between the haplotype at the -54 bp position of the *OsWOX13* gene promoter (Chr 1: 34863184) and heading date in natural populations. The total number of varieties was 2792. The frequencies of the *Hap-T* and *Hap-C* were 33.7% and 64.4%, respectively, whereas *Hap-Y*, corresponding to the heterozygous genotype, exhibited a frequency of 1.9%. Statistical significance of heading date between rice varieties carrying *Hap-T* and those carrying *Hap-C* was analyzed using a two-tailed Student's *t* test. (*P* = 4.64E-05). **B** and **C)** Heading dates were calculated for Longjing 31, Longjing $31^{T\text{-}C}$-1 and Longjing $31^{T\text{-}C}$-2 under CLD (**B**) and CSD (**C**). Longjing $31^{T\text{-}C}$ represents the genotype where the thymine (T) residues at positions 34863184 and 34863187 on chromosome 1 are both mutated to cytosine (C). Data are means ± SD (n = 30 plants). Statistical analysis was performed using ANOVA followed by Tukey's test ($P<0.05$). **D)** Structure diagram of recombinant vector. The *Pro35S:*REN-*OsWOX13-P1T*-LUC and *Pro35S:*REN-*OsWOX13-P1C*-LUC constructs serve as reporters, while the *Pro35S:Ehd1-FLAG* and *Pro35S:FLAG* construct serves as effectors, respectively. **E)** The LUC assay analyzed the activation ability of Ehd1 on *OsWOX13* promoters with different haplotypes. Both *OsWOX13-P1T* and *OsWOX13-P1C* encompass the 2000 bp upstream sequence of the *OsWOX13* promoter, with *OsWOX13-P1T* harboring a T and *OsWOX13-P1C* a C at the -54 bp position (Chr 1: 34863184). HSP82 as the internal reference protein. Statistical analysis was performed using ANOVA followed by Tukey's test ($P<0.05$). Data are means ± SD (n = three independent experiments). **F)** The EMSA assay analyzed the binding ability of Ehd1 on *OsWOX13* promoters with different haplotypes (n = three independent experiments). The sequences of labeled probes *P2-2* and *P2-2-T* were identical, with a T at the -54 bp position, whereas labeled probes *P2-2-C* differed only at the -54 bp position, where it had a C. **G** to **N)** The expression levels of *OsWOX13* and *Hd3a* in different haplotypes were analyzed (n = three biological replicates). Forty rice varieties each of *Hap-T* and *Hap-C* were randomly selected. After being grow for 25 days under CSD conditions and 50 days under CLD conditions, the expression levels of *OsWOX13* (**G** and **H**) and *Hd3a* (**I** and **J**) in leaves were determined by qRT-PCR. Data are means ± SD (n = 40 plants). Longjing 31, Longjing $31^{T\text{-}C}$-1 and Longjing $31^{T\text{-}C}$-2 were grown under CSD and CLD for 35 and 45 days, respectively, followed by the determination of the expression levels of *OsWOX13* (**K** and **L**) and *Hd3a* (**M** and **N**) in leaves. The relative expression levels of *OsWOX13* and *Hd3a* were assessed using $2^{-\Delta\Delta CT}$ method. Data are presented as mean ± SD (n = three biological replicates). Statistical analysis was performed using two-tailed Student's *t* test (**G** to **J**) and ANOVA followed by Tukey's test ($P<0.05$) (**K** to **N**).

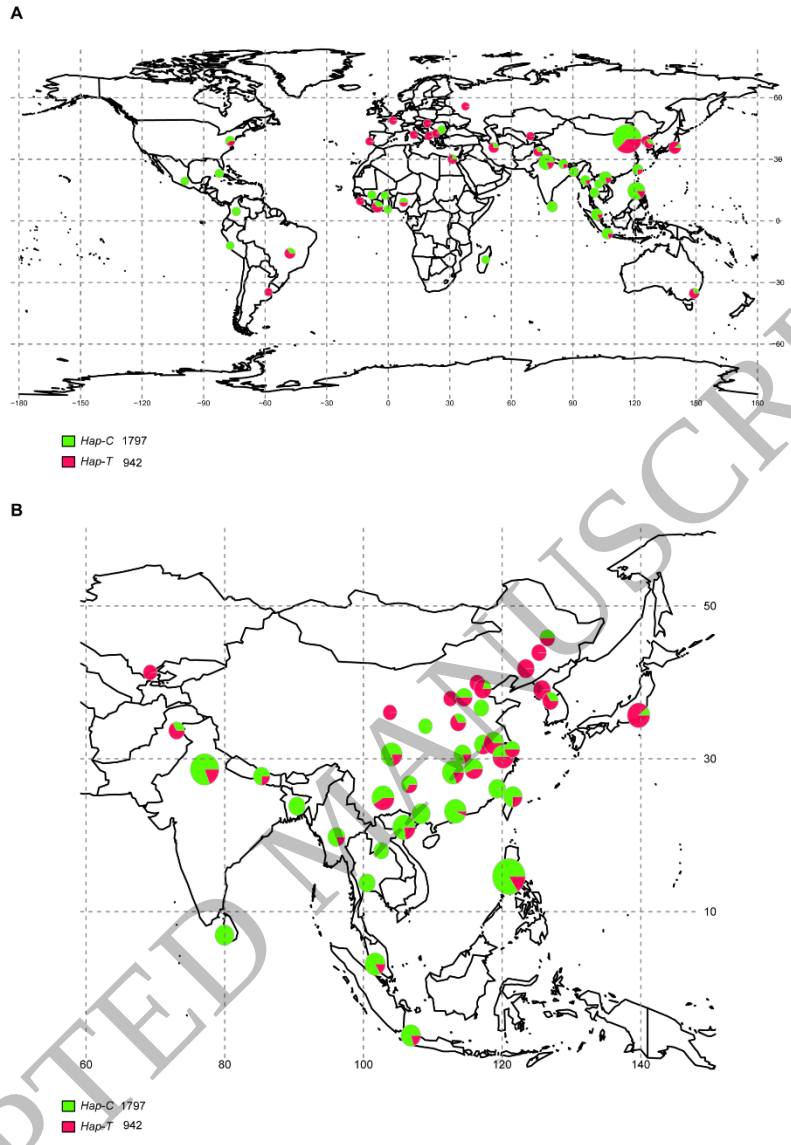

Figure 7. The geographical distribution of *Hap-T* and *Hap-C*. **A** and **B)** The geographical distribution of the two haplotypes, *Hap-T* and *Hap-C*, was investigated worldwide and across Asia. The sample sizes for the *Hap-T* and *Hap-C* were 942 and 1797 rice accessions, respectively. Green indicates the presence of the *Hap-C* haplotype, while red represents the *Hap-T* haplotype. Pie charts were used to illustrate the proportions of *Hap-T* and *Hap-C* haplotypes. The dotted lines represent longitude and latitude.

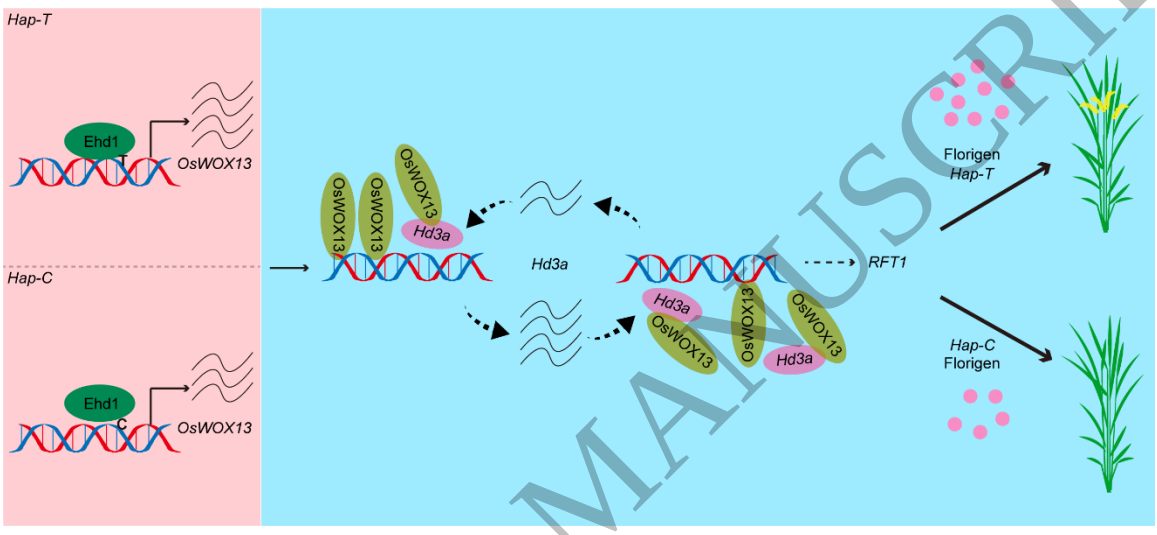

Figure 8. Model of *Ehd1-OsWOX13-Hd3a* pathway regulation of heading date in rice. Ehd1 exhibits a stronger activation effect on *OsWOX13* expression in the *Hap-T*. OsWOX13 binds to the *Hd3a* promoter and activates its expression; moreover, the interaction between OsWOX13 and Hd3a weakens the activation of *Hd3a* expression, that precisely modulates *Hd3a* transcription and indirectly regulates the level of *RFT1*. Ultimately, *OsWOX13* in the *Hap-T* shows higher expression, leading to elevated florigen levels and thus promoting heading in rice.